

EFFECTS OF THE PLANT PHENOLIC QUERCETIN ON PROTEIN
AND mRNA EXPRESSIONS OF XENOBIOTIC METABOLIZING
CYP1A1, CYP2E1, NQO1 AND GST ENZYMES IN COLON CANCER
CELL LINE SW620

A THESIS SUBMITTED TO
THE GRADUATE SCHOOL OF NATURAL AND APPLIED SCIENCES
OF
MIDDLE EAST TECHNICAL UNIVERSITY

BY

MELİHA ÜLGER

IN PARTIAL FULFILLMENT OF THE REQUIREMENTS
FOR
THE DEGREE OF MASTER OF SCIENCES
IN
BIOCHEMISTRY

JULY 2015

Approval of the Thesis:

**EFFECTS OF THE PLANT PHENOLIC QUERCETIN ON PROTEIN AND
mRNA EXPRESSIONS OF XENOBIOTIC METABOLIZING CYP1A1,
CYP2E1, NQO1 AND GST ENZYMES IN COLON CANCER CELL LINE
SW620**

submitted by **MELİHA ÜLGER** in partial fulfillment of the requirements
for the degree of the degree of **Master of Science in Biochemistry
Department, Middle East Technical University** by,

Prof. Dr. Gülbin Dural Ünver _____
Dean, Graduate School of **Natural and Applied Sciences**

Prof. Dr. Orhan Adalı _____
Head of Department, **Biochemistry**

Prof. Dr. Orhan Adalı _____
Supervisor, **Biology Dept., METU**

Assoc. Prof. Dr. Ayşe Mine Gençler Özkan
Co-Supervisor, **Faculty of Pharmacy, Ankara University**

Examining Committee Members: _____

Prof. Dr. Tülin Güray _____
Biology Dept., METU

Prof. Dr. Orhan Adalı _____
Biology Dept., METU

Prof. Dr. Özlem Yıldırım Esen _____
Biology Dept., Ankara University

Assoc. Prof. Dr. Ayşe Mine Gençler Özkan _____
Faculty of Pharmacy, Ankara University

Assoc. Prof. Dr. Nursen Çoruh _____
Chemistry Dept., METU

Date: 31.07.2015

I hereby declare that all information in this document has been obtained and presented in accordance with academic rules and ethical conduct. I also declare that, as required by these rules and conduct, I have fully cited and referenced all material and results that are not original to this work.

Name, Last Name: Meliha Ülger

Signature:

ABSTRACT

EFFECTS OF THE PLANT PHENOLIC QUERCETIN ON PROTEIN AND mRNA EXPRESSIONS OF XENOBIOTIC METABOLIZING CYP1A1, CYP2E1, NQO1 AND GST ENZYMES IN COLON CANCER CELL LINE SW620

Ülger, Meliha

M.S., Department of Biochemistry

Supervisor : Prof. Dr. Orhan Adalı

Co-supervisor : Assoc. Prof. Dr. Ayşe Mine Gençler Özkan

July 2015, 95 pages

Quercetin has been one of the most studied flavonoids for years because of its widespread effects on various health problems and is known to be a potent anti-carcinogenic compound. One possible mechanism that flavonoids may prevent or treat cancer is by regulation of phase I and phase II enzyme activity. Phase I enzymes are xenobiotic metabolizing cytochrome P450 (CYP) enzymes whose functions are activating or inactivating xenobiotic compounds. CYP1A1 and CYP2E1 enzymes are actively found on cancer cells and modify carcinogenic compounds. Phase II enzymes are responsible from conjugation reactions in the body. GSTP1 and NQO1 enzymes are important representatives of phase II enzymes and their function is elimination of possibly carcinogenic metabolites by

reduction and conjugation reactions. This study focused on the effects of quercetin on CYP1A1, CYP2E1, GSTP1 and NQO1 enzymes in human colon carcinoma cell line SW620. In order to study these effects, cells were grown as in 5% CO₂ incubator prior to the treatment with quercetin with respect to IC₅₀ value that is determined as 90 μM, and then the effects of quercetin on protein and mRNA expressions are analyzed according to the control groups by Western Blotting and q-RT-PCR, respectively.

Quercetin treatment caused 47 % decrease in CYP1A1 protein expression (p<0.01) and 17 % decrease in CYP2E1 protein expression (p<0.01). Furthermore, quercetin treatment caused 85 % decrease in CYP1A1 mRNA expression and 97 % decrease in CYP2E1 mRNA expression with respect to control cells and results are normalized with GAPDH as an internal reference. Moreover, quercetin treatment also caused 35 % decrease in GSTP1 protein expression (p<0.001) and 29 % decrease in NQO1 protein expression (p<0.001). In addition, quercetin treatment caused 75 % decrease in GSTP1 mRNA expression (p<0.05), whereas NQO1 mRNA expression is increased 1.6 fold (p<0.01) after quercetin treatment.

In conclusion, the results of this study showed that plant phenolic quercetin can modulate the progression of colon carcinoma by affecting the expression of protein and mRNA of xenobiotic metabolizing phase I and phase II enzymes CYP1A1, CYP2E1, GSTP1 and NQO1.

Keywords: Quercetin, SW620, Cytochrome P450, CYP1A1, CYP2E1, GSTP1, NQO1, carcinogen, Western Blot, qRT-PCR, mRNA and protein expression.

ÖZ

BİTKİ FENOLİĞİ KERSETİNİN SW620 KOLON KARSİNOMA HÜCRE HATTINDA KSENOBİYOTİK METABOLİZE EDEN CYP1A1, CYP2E1, NQO1 VE GST ENZİMLERİNİN PROTEİN VE mRNA EKPREZYONLARINA ETKİSİ

Ülger, Meliha

Yüksek Lisans, Biyokimya Bölümü

Tez Yöneticisi: Prof. Dr. Orhan Adalı

Ortak Tez Yöneticisi: Doç. Dr. Ayşe Mine Gençler Özkan

Temmuz 2015, 95 sayfa

Kersetin çeşitli sağlık problemleri üzerindeki yaygın etkisi dolayısıyla yıllardır en çok çalışılan flavonoidlerden biridir ve etkili bir anti karsinojen bileşik olduğu bilinmektedir. Flavonoidlerin kanseri önleyebileceği veya tedavi edebileceği muhtemel mekanizmalarından biri faz I ve faz II enzim aktivitelerini düzenlemektir. Faz I enzimleri, ksenobiyotik bileşiklerin aktivasyon veya deaktivasyonundan sorumlu olan ksenobiyotik metabolize eden enzimlerdir ve sitokrom P450 enzimleri bu sınıfa dahildir. CYP1A1 ve CYP2E1 enzimleri kanser hücrelerinde aktif olarak bulunurlar ve karsinojenik bileşikleri modifiye ederler. Faz II enzimleri vücutta konjugasyondan sorumludurlar. GSTP1 ve NQO1 enzimleri faz II enzimlerinin önemli temsilcileridir ve görevleri, potansiyel karsinojenik

metabolitlerin indirgenme ve konjugasyon reaksiyonları aracılığıyla eliminasyonudur. Bu çalışma kersetinin SW620 kolon karsinoma hücre hattında CYP1A1, CYP2E1, GSTP1 ve NQO1 enzimleri üzerine etkileri üzerine odaklanmıştır. Bu etkileri çalışabilmek için hücreler %5 CO₂ içeren inkubatörde büyütülmüş ve akabinde 90 µM olarak bulunmuş olan IC50 değerine uygun olarak kersetinle muamele edilmiş ve bunu takiben kersetinin protein ve mRNA ekspresyonları üzerine etkileri sırasıyla Western Blot ve q-RT-PCR teknikleri ile analiz edilmiştir.

Mevcut çalışmanın sonuçlarına göre, kersetin muamelesi CYP1A1 protein ekspresyonunda % 47 (p<0.01), CYP2E1 protein ekspresyonunda ise % 17 (p<0.01) azalmaya sebep olmuştur. Ayrıca, kersetin muamelesi sonucunda GAPDH mRNA sonuçları ile normalize edilmiş CYP1A1 mRNA ekspresyonu % 85 azalırken, CYP2E1 mRNA ekspresyonu da % 97 azalmıştır. Bunun yanı sıra, kersetin muamelesi sonucu GSTP1 protein ekspresyonu % 35 (p<0.001), NQO1 protein ekspresyonu da % 29 (p<0.001) azalma göstermiştir. Kersetin muamelesi, GSTP1 mRNA ekspresyonunu % 75 azaltırken (p<0.05) NQO1 mRNA ekspresyonunu da 1,6 kat artırmıştır (p<0.01).

Sonuç olarak, mevcut çalışmanın sonuçları bitki fenoliği kersetinin ksenobiotik metabolize eden faz I ve faz II enzimleri CYP1A1, CYP2E1, GSTP1 ve NQO1 protein ve mRNA ekspresyonlarını etkileyerek kolon kanseri ilerleyişini düzenleyebileceğini göstermiştir.

Anahtar kelimeler: Kersetin, SW620, Sitokrom P450, CYP1A1, CYP2E1, GSTP1, NQO1, Karsinogen, Western Blot, qRT-PCR, mRNA ve protein ekspresyonu.

To My Family,

For their endless love and support

ACKNOWLEDGEMENTS

I am deeply grateful to my supervisor Prof. Dr. Orhan Adalı for his valuable guidance, patient, continued advice and critical discussion, his kindness and generosity throughout this study.

I am also deeply grateful to my co-supervisor Assoc. Prof. Dr. Ayşe Mine Gençler Özkan for her guidance and advices throughout this study.

I thank to my examining committee members Prof. Dr. Tülin Güray, Prof. Dr. Özlem Yıldırım Esen and Assoc. Prof. Dr. Nursen Çoruh for their suggestions and criticism.

I am very grateful to Dr. Serdar Karakurt and Tuba Çulcu from whom I have learned a lot before and throughout the study.

I would like to thank all my labmates Emre Evin, Merve Akkulak, Özlem Durukan, Sena Gjota, Ezgi Balkan, Zekiye Ceren Arıtuluk and Tuğçe Öner for their beautiful friendship and support. It was enjoyable to work with them.

I am also grateful to my parents my brother for their permanent encouragement and belief in me throughout this work. Their help, advice, patience, support, and love are undeniable and unforgettable.

Finally I would like to express my warmest thanks to my fiancé Ömer Yılmaz who has worked even harder than me throughout this study just to make me feel better and I am deeply grateful for his endless love and care.

This study is dedicated to my family. Without their love, support and patience I couldn't have come this far. Thank you for everything.

TABLE OF CONTENTS

ABSTRACT	v
ÖZ	vii
ACKNOWLEDGEMENTS.....	x
TABLE OF CONTENTS	xi
LIST OF TABLES.....	xiv
LIST OF FIGURES	xv
LIST OF SYMBOLS AND ABBREVIATIONS	xx
CHAPTER 1	1
INTRODUCTION	1
1.1. Phenolic Compounds	1
1.1.1. Flavonoids	1
1.1.1.1 Quercetin	4
1.2 Phase I and Phase II Xenobiotic Metabolizing Enzymes	5
1.2.1 Phase I Xenobiotic Metabolizing Enzymes.....	6
1.2.2 Phase II Xenobiotic Metabolizing Enzymes	17
1.3 Aim of the Study	22
CHAPTER 2	25
MATERIALS AND METHODS	25
2.1 Materials 25	
2.1.1 Cell Line	25
2.1.2 Chemicals and Materials	25

2.2 Methods.....	27
2.2.1 Cell Culture	27
2.2.2 Protein Extraction	30
2.2.3 Determination of Protein Concentration.....	30
2.2.4 Determination of Protein Expression.....	32
2.2.5 Determination of mRNA Expression.....	38
2.2.5.1 Isolation of Total RNA from Cell Lines	38
2.2.5.2 Determination of RNA Concentration	39
2.2.5.3 Qualification of RNA Molecules by Agarose Gel Electrophoresis	39
2.2.5.4 cDNA Synthesis	40
2.2.5.5 Quantitative Real-Time PCR	40
2.2.6 Statistical Analysis.....	43
CHAPTER 3.....	45
RESULTS.....	45
1. 3.1 Cell Culture.....	45
2. 3.1.1 IC50 Determination	45
3.2. Protein Concentrations of Lysates of the Control and the Treated Cells 48	
3.3 Protein Expression Analysis of CYP1A1, CYP2E1, NQO1 and GSTP1 Enzymes in SW620 Cells.....	49
3.3.1 CYP1A1 Protein Expression in the Control and the Quercetin Treated Cells	49
3.3.2 CYP2E1 Protein Expression in the Control and the Quercetin Treated Cells	51

3.3.3 GSTP1 Protein Expression in the Control and the Quercetin Treated Cells.....	52
3.3.4 NQO1 Protein Expression in the Control and the Quercetin Treated Cells.....	54
3.4 CYP1A1, CYP2E1, NQO1 and GSTP1 mRNA Expressions in the Control and Quercetin Treated SW620 Cells	56
3.4.1 Quality Control of RNA Molecules by Agarose Gel Electrophoresis	56
3.4.2 CYP1A1 mRNA Expression in the Control and the Quercetin Treated SW620 Cells.....	57
3.4.3 CYP2E1 mRNA Expression in the Control and the Quercetin Treated SW620 Cells.....	62
3.4.4 GSTP1 mRNA Expression in the Control and the Quercetin Treated SW620 Cells.....	66
3.4.5 NQO1 mRNA Expression in the Control and the Quercetin Treated SW620 Cells.....	70
CHAPTER 4	75
DISCUSSION.....	75
CHAPTER 5	81
CONCLUSION	81
REFERENCES	83

LIST OF TABLES

TABLES

Table 1.1 Structures of the most common subclasses of flavonoids and their food sources (Bondonno et al., 2015).....	3
Table 1.2 CYP families and functions in human (Nelson, 2009).....	9
Table 1.3 Substrates, inducers and inhibitors of CYP2E1 (Modified from “Drug Interactions: Cytochrome P450 Drug Interaction Table” in by Flockhart DA, 2007).....	16
Table 2.1 Constituents of separating and stacking gel solutions for two gels.....	33
Table 2.2 Primer sequences, annealing temperatures and product sizes of the genes.	42
Table 3.1 Percent AB reduction and percent survival values of the cells	46
Table 3.2 Average protein concentrations of whole cell lysates of control and treated cells.	49
Table 3.3 The Livak method for the calculation of relative mRNA expression using Ct values.	61
Table 4.1 Summary of the protein and mRNA expression analysis results for CYP1A1, CYP2E1, GSTP1 and NQO1 from control and quercetin treated cells.....	77

LIST OF FIGURES

FIGURES

Figure 1.1 General flavonoid structure and labeling (Percival et al., 1998).....	2
Figure 1.2 Structure of quercetin.	4
Figure 1.3 The catalytic cycle of cytochrome P450 (Guengerich, 2001).....	8
Figure 1.4 3-D crystal structure of human CYP1A1 (Walsh et al., 2013).	10
Figure 1.5 Metabolic activation of B[a]P and 7,12-DMBA to the carcinogenic metabolites (Androutsopoulos, 2009).	12
Figure 1.6 Stereo views of CYP 2E1 active site showing the ligand containing active site, small distal void, and access channel (Porubsky, 2008).....	14
Figure 1.7 3-D structure of GST enzyme (Wu and Dong, 2012).	18
Figure 1.8 Conjugation reaction catalyzed by GST enzymes (Magoma, 2013).....	19
Figure 1.9 3-D structure of NQO1 enzyme. Red and blue areas represent N-terminal domain, whereas yellow and green areas represents C-terminal domain (Gad Asher, 2006).	20
Figure 1.10 Ping-pong enzymatic mechanism of NQO1 (Ross et al., 1994).	21
Figure 2.1 Western blot sandwich	37
Figure 3.1 Color shift among wells after AB assay following quercetin treatment ranging from 25 μ M to 200 μ M.....	45
Figure 3.2 Cell proliferation graph for quercetin treated cells.	47
Figure 3.3 Percent survival graph for quercetin treated cells.	47
Figure 3.4 Control (A) and 90 μ M (IC ₅₀ value) quercetin treated (B) wells prior to protein extraction.	48
Figure 3.5 Immunoreactive protein bands of control and quercetin treated SW620 cells representing the expression of CYP1A1 (58 kDa). GAPDH (37	

kDa) used as internal standard. Lane 1-3: Control, Lane 4-6: Quercetin Treated Cells. Each well is loaded with 20 mg protein. 50

Figure 3.6 Comparison of CYP1A1 protein expression of control and quercetin treated cells. The band quantifications are expressed as mean \pm SD and experiments were carried out in triplicate. Statistical analysis of CYP1A1 protein expression was done by unpaired, two-tailed student's t-test and ** means $P \leq 0.01$ 50

Figure 3.7 Immunoreactive protein bands of control and quercetin treated SW620 cells representing the expression of CYP2E1 (52 kDa). GAPDH (37 kDa) used as internal standard. Lane 1-3: Control, Lane 4-6: Quercetin Treated Cells. Each well is loaded with 20 mg protein. 51

Figure 3.8 Comparison of CYP2E1 protein expression of control and quercetin treated cells. The band quantifications are expressed as mean \pm SD and experiments were carried out in triplicate. Statistical analysis of CYP2E1 protein expression was done by unpaired, two-tailed student's t-test and ** means $P \leq 0.01$ 52

Figure 3.9 Immunoreactive protein bands of control and quercetin treated SW620 cells representing the expression of GSTP1 (23 kDa). GAPDH (37 kDa) used as internal standard. Lane 1-3: Control, Lane 4-6: Quercetin Treated Cells. Each well is loaded with 20 mg protein. 53

Figure 3.10 Comparison of GSTP1 protein expression of control and quercetin treated cells. The band quantifications are expressed as mean \pm SD and experiments were carried out in triplicate. Statistical analysis of GSTP1 protein expression was done by unpaired, two-tailed student's t-test and ** means $P \leq 0.01$ 54

Figure 3.11 Immunoreactive protein bands of control and quercetin treated SW620 cells representing the expression of NQO1 (31 kDa). GAPDH (37 kDa) used as internal standard. Lane 1-3: Control, Lane 4-6: Quercetin Treated Cells. Each well is loaded with 20 mg protein. 55

Figure 3.12 Comparison of NQO1 protein expression of control and quercetin treated cells. The band quantifications are expressed as mean \pm SD and experiments were carried out in triplicate. Statistical analysis of NQO1

protein expression was done by unpaired, two-tailed student's t-test and *** means $P \leq 0.001$56

Figure 3.13 Agarose gel electrophoresis results of RNA samples isolated from quercetin treated (Lane 1) and control (Lane 2) cells. 10 μ l RNA samples were loaded in each well.....57

Figure 3.14 Standard curve generated from serial dilutions of control cDNA to calculate quantities of CYP1A1 mRNAs in the control and quercetin treated cells relatively.58

Figure 3.15 Amplification curve showing the accumulation of fluorescence emission at each reaction cycle.....58

Figure 3.16 Melting curve showing the fluorescence emission change versus temperature. Detection of single peak means single PCR product..... 59

Figure 3.17 qRT-PCR products of CYP1A1 cDNA (121bp) of control (Lane 3-5) and quercetin treated (Lane 6-8) cells. 5 μ L of qRT-PCR product was loaded in each well. Lane 1 shows the bp markers and NTC (Lane 2) is the no template control. 60

Figure 3.18 qRT-PCR products of GAPDH cDNA (197bp) of control (Lane 3-5) and quercetin treated (Lane 6-8) cells. 5 μ L of qRT-PCR product was loaded in each well. Lane 1 shows the bp markers and NTC (Lane 2) is the no template control. 60

Figure 3.19 Comparison of CYP1A1 mRNA expressions between control and quercetin treated cells. The quantities are expressed as mean \pm SD of the relative expression. Experiments were carried out in triplicate. Statistical analysis of CYP1A1 mRNA expression was done by unpaired, two-tailed student's t-test..... 62

Figure 3.20 Standard curve generated from serial dilutions of control cDNA to calculate quantities of CYP2E1 mRNAs in the control and quercetin treated cells relatively. 63

Figure 3.21 Amplification curve showing the accumulation of fluorescence emission at each reaction cycle..... 64

Figure 3.22 Melting curve showing the fluorescence emission change versus temperature. Detection of single peak means single PCR product..... 64

Figure 3.23 qRT-PCR products of CYP2E1 cDNA (184bp) of control (Lane 3-5) and quercetin treated (Lane 6-8) cells. 5 μ L of qRT-PCR product was loaded in each well. Lane 1 shows the bp markers and NTC (Lane 2) is the no template control. 65

Figure 3.24 Comparison of CYP2E1 mRNA expressions between control and quercetin treated cells. The quantities are expressed as mean \pm SD of the relative expression. Experiments were carried out in triplicate. Statistical analysis of CYP2E1 mRNA expression was done by unpaired, two-tailed student's t-test. 66

Figure 3.25 Standard curve generated from serial dilutions of control cDNA to calculate quantities of GSTP1 mRNAs in the control and quercetin treated cells relatively. 67

Figure 3.26 Amplification curve showing the accumulation of fluorescence emission at each reaction cycle. 67

Figure 3.27 Melting curve showing the fluorescence emission change versus temperature. Detection of single peak means single PCR product. 68

Figure 3.28 qRT-PCR products of GSTP1 cDNA (137bp) of control (Lane 3-5) and quercetin treated (Lane 6-8) cells. 5 μ L of qRT-PCR product was loaded in each well. Lane 1 shows the bp markers and NTC (Lane 2) is the no template control. 69

Figure 3.29 Comparison of GSTP1 mRNA expressions between control and quercetin treated cells. The quantities are expressed as mean \pm SD of the relative expression. Experiments were carried out in triplicate. Statistical analysis of GSTP1 mRNA expression was done by unpaired, two-tailed student's t-test and * means $P \leq 0.05$ 70

Figure 3.30 Standard curve generated from serial dilutions of control cDNA to calculate quantities of NQO1 mRNAs in the control and quercetin treated cells relatively. 71

Figure 3.31 Amplification curve showing the accumulation of fluorescence emission at each reaction cycle. 71

Figure 3.32 Melting curve showing the fluorescence emission change versus temperature. Detection of single peak means single PCR product. 72

Figure 3.33 qRT-PCR products of NQO1 cDNA (196bp) of control and treated cells. 5 μ L of qRT-PCR product was loaded in each well. NTC is the no template control. 73

Figure 3.34 Comparison of NQO1 mRNA expressions between control and quercetin treated cells. The quantities are expressed as mean \pm SD of the relative expression. Experiments were carried out in triplicate. Statistical analysis of NQO1 mRNA expression was done by unpaired, two-tailed student's t-test. ** means $P \leq 0.01$ 74

LIST OF SYMBOLS AND ABBREVIATIONS

AhR	Aryl Hydrocarbon Receptor
APS	Ammonium per sulfate
ARNT	aryl hydrocarbon receptor nuclear translocator
B[a]P	Benzo[a]pyrene
BCIP	5-bromo 4-chloro 3-indoyl phosphate
BSA	Bovine serum albumin
BCA	Bicinchoninic acid
cDNA	Complementary DNA
Ct	Threshold cycle
CYP	Cytochrome P450
DEPC	Diethylpyrocarbonate
DMSO	Dimethyl sulfoxide
DNA	Deoxyribonucleic acid
dNTP	Deoxynucleoside triphosphate
DTT	Dichlorodiphenyltrichloroethane
EDTA	Ethylenediaminetetraacetic acid
ERB	Electronic running buffer
FAD	Flavin adenine dinucleotide
FBS	Fetal bovine serum
FMO	Flavin-containing monooxygenase
GAPDH	Glyceraldehyde-3-phosphate dehydrogenase
GST	Glutathione S-transferase
HAH	Halogenated aromatic hydrocarbons
HRP	Horseradish peroxide
HSP90	90-kDa heat-shock proteins
IC50	Half maximal inhibitory concentration
kDa	Kilo Dalton

mRNA	Messenger RNA
NADH	Nicotinamide adenine dinucleotide, reduced form
NADPH	Nicotinamide adenine dinucleotide phosphate, reduced form
NBT	Nitrotetrazolium blue chloride
NF-kB	Nuclear factor-kappaB
NQO1	NAD(P)H: Quinone Oxidoreductase I
OD	Optical density
PAH	Polycyclic aromatic hydrocarbon
PBS	Phosphate buffered saline
PCR	Polymerase chain reaction
Pen-Strep	Penicillin-Streptomycin
PMSF	Phenylmethylsulfonyl fluoride
rpm	Revolutions per minute
RNA	Ribonucleic acid
ROS	Reactive Oxygen Species
SDB	Sample dilution buffer
SDS	Sodium dodecyl sulfate
SDS-PAGE	Sodium dodecyl sulfate-polyacrylamide gel electrophoresis
TBST	Tris-buffered saline and Tween 20
TEMED	Tetramethylethylenediamine

CHAPTER 1

INTRODUCTION

1.1. Phenolic Compounds

Phenolic compounds are a large class of plant secondary metabolites, showing a diversity of structures, from rather simple structures, through polyphenols such as flavonoids, which comprise several groups, to polymeric compounds. Phenolic compounds are important for the quality of plant based foods and also they give the color of red fruits, juices and wines. In addition, they are considered to contribute to the health benefits associated to dietary consumption of fruits and vegetables. Flavonoids are one of the main classes of phenolic compounds.

1.1.1. Flavonoids

Flavonoids belong to a group of secondary metabolites with variable phenolic structures and are found in fruit, vegetables, grains, bark, roots, stems, flowers, tea, and wine (Middleton et al., 1998). Flavonoids are important components of the human diet, and are the most widely distributed phenolic compounds in plant foods and also the most studied ones. Studies show that flavonoids are among the most effective antioxidants from plants (Pandey et al., 2009). Their excellent antioxidant activity is related to the presence of hydroxyl groups in positions 3' and 4' of the B ring (Figure 1.1).

These groups give high stability to the formed radical by participating in the displacement of the electron, and a double bond between carbons C₂ and C₃ of the ring C together with the carbonyl group at the C₄ position, which makes the displacement of an electron possible from the ring B (Percival et al., 1998). Figure 1.1 represents general flavonoid structure and numbering.

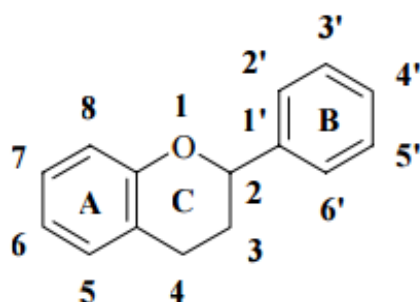
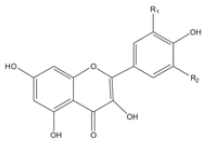
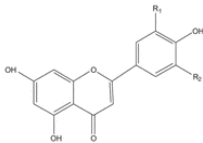
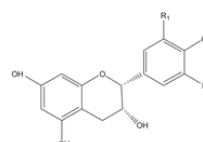
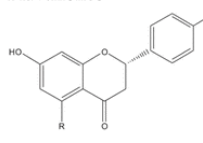
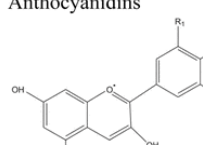
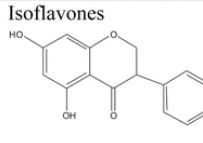


Figure 1.1 General flavonoid structure and labeling (Percival et al., 1998).

Flavonoids can be divided into various classes on the basis of their molecular structure. Table 1.1 represents the structures of the most common subclasses of flavonoids and their food sources.

Table 1.1 Structures of the most common subclasses of flavonoids and their food sources (Bondonno et al., 2015).

Subclass	Prominent flavonoids	Typical food source
Flavonols 	Isorhamnetin Kaempferol Quercetin Myricetin	Tea, apples, onions, curly kale, leeks, broccoli, blueberries, red wine
Flavones 	Apigenin Luteolin	Parsley, celery
Flavan-3-ols 	(+)-Catechin (+)-Gallocatechin (-)-Epicatechin (-)-Epigallocatechin (-)-Epicatechin-3-gallate (-)-Epigallocatechin-3-gallate	Tea, red wine, red grapes, cocoa, chocolate, apricots
Flavanones 	Eriodictyol Hesperetin Naringenin	Citrus fruit, tomatoes, mint
Anthocyanidins 	Cyanidin Delphinidin Malvidin Pelargonidin Petunidin Peonidin	Berries, red wine
Isoflavones 	Daidzein Genistein Glycitein	Soybeans, soy foods, legumes

More than 5000 varieties of flavonoids have been identified and many of them are used in various studies. This research will focus on one of the most common dietary flavonoid quercetin, which belongs to the subclass flavonol.

1.1.1.1 Quercetin

Quercetin (3,3',4',5,7-pentahydroxyflavone) belongs to an extensive class of polyphenolic flavonoid compounds and it is the most prominent dietary flavonol. Figure 1.2 represents the structure of quercetin. It is ubiquitously present in foods including vegetables, fruit, tea and wine. The daily intake of quercetin in Western countries has been estimated as 25-50 mg/day, whereas total flavonoid intake of approximately 1 g/day (Hollman et al., 1997). A detailed estimation of consumption in Western diets found the richest sources of quercetin to be onions (347 mg/kg), apples (36 mg/kg), and red wine (11 mg/kg) (Hertog et al., 1993).

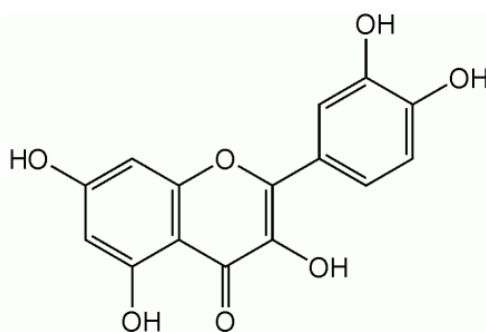


Figure 1.2 Structure of quercetin.

Quercetin has been one of the most studied flavonoids for years because of its widespread effects on various health problems. Several studies showed that quercetin has a protective role in breast, lung, liver, ovarian, and colorectal cancers (Scambia, 1994; Huber et al., 1997; Denda et al., 1998; Khanduja et al., 1999; Choi et al., 2001). This anti-carcinogenic effect may be due to one of several mechanisms that quercetin has been shown to exert on cancer cells. These mechanisms include: antioxidant activity, anti-inflammatory action, stimulation of apoptosis, decreased cell proliferation,

and regulation of xenobiotic metabolizing Phase I and Phase II enzyme activities (Bravo, 1998; Nijveldt et al., 2001).

The flavonoids are a class of polyphenols and their structure includes two phenolic benzene rings linked by a heterocyclic pyrone ring containing an oxygen molecule as given previously in Figure 1.1. In nature, almost all flavonoids are found in the glycosylated form, which means they are linked to a sugar moiety. Quercetin belongs to a class of flavonoids called flavonols, which are characterized by a 3-OH group on the pyrone ring (Figure 1.2) (Sampson et al., 2002).

Many studies indicate that the structure of quercetin is directly responsible for its functions. Only nonpolar flavonoids with free hydroxyl groups, such as quercetin, showed anti-carcinogenic properties (Siess et al., 2000). In some other studies, it has been shown that quercetin modulates the activity of drug metabolizing enzymes, which are important in the prevention of colon cancer (Guengerich, 1992). Quercetin like flavonoids, which have free hydroxyl groups, inhibit Phase I enzyme activity, and flavonoids without free hydroxyl groups, stimulate Phase I enzyme activity (Yang et al., 1992).

1.2 Phase I and Phase II Xenobiotic Metabolizing Enzymes

Humans are constantly exposed to potential carcinogens – through air, water, foods and any kind of pollution. One of the most important mechanisms used by the body to deal with these potential carcinogens is a system of xenobiotic metabolizing enzymes. This system composed of two separate classes of enzymes: the Phase I enzymes and the Phase II enzymes. These two enzyme groups operate together due to metabolize any xenobiotic, which make contact with the body. The Phase I and Phase II enzymes are crucial to the body's defense against cancer, and several studies

recently have focused on how activity of these enzymes and their concentrations in the body influence the risk of cancer (Cheung and Kong, 2009). These two classes of enzymes work in cooperation, and each is necessary to eliminate the carcinogens from the body. Since vast majority of the xenobiotic compounds are in the hydrophobic form, their conversion to the hydrophilic form by the Phase I and Phase II enzymes is essential in order to excretion from the body (Jones and DeLong, 2000).

1.2.1 Phase I Xenobiotic Metabolizing Enzymes

Phase I reactions convert lipophilic xenobiotic compounds into more readily excreted hydrophilic products. These conversions occur by oxidation, reduction, hydrolysis, cyclization, decyclization, addition of oxygen or removal of hydrogen and they performed by mixed function oxidases (MFOs), often in the liver. These reactions mainly serve as detoxification reactions in the body.

The most of the phase I transformation reactions are carried out by a family of enzymes called the cytochrome P450 monooxygenases (CYPs). CYPs are the most remarkable phase I enzyme family since they catalyze the conversion of several xenobiotic compounds to the products, which are biologically active. This system serves as both a detoxification route and a metabolic activation route that yields reactive metabolites which initiate toxic and carcinogenic events (Arınc et al., 1991, 2000a, 2000b). Aside from CYPs, any other enzymes contribute to the phase I process include the flavine monooxygenases (FMOs) (Halpert et al., 1998; Adalı et al., 1998); alcohol and aldehyde dehydrogenases, and monoamine oxidases (MAO's).

1.2.1.1 Cytochrome P450s

Cytochrome P450 (CYP) monooxygenases are the largest and best studied group of phase I enzymes. They are a superfamily of heme-enzymes essential for the oxidative, peroxidative, and reductive metabolism of a various compounds, including endobiotics, such as steroids, bile acids, fatty acids, prostaglandins, Vitamin D and xenobiotics, comprising most of the therapeutic drugs, pesticides, food additives, environmental pollutants (Nelson et al. 1996, Bertz & Granneman 1997). The first report on the existence of a CYP enzyme was published in 1958 by Klingenberg et al. Since this enzyme gave a unique 450- nm optical absorption peak when its hemoprotein nature was recognized, it was given the name cytochrome P450 (Omura, 1999).

Eukaryotic CYPs are membrane-bound, mostly localized to the endoplasmic reticulum (ER), but some CYPs are also present in mitochondrial inner membranes. The active site of cytochrome P450 contains a heme-iron center. In order to function, cytochrome P450s require an electron transfer chain. In the ER, this source is NADPH-cytochrome P450 reductase (Omura, 1999). Lipid is involved in the transfer of electrons from NADPH cytochrome P450 reductase to cytochrome P450 in the monooxygenase system.

To initiate the cycle, substrate binds in proximity to the ferric (Fe^{+3}) heme group and induces electron transfer from NAD(P)H via cytochrome P450 reductase (Figure 1.3). In the next step, molecular oxygen (O_2) binds to the resulting ferrous (Fe^{+2}) heme center. Then a second electron is transferred from cytochrome P450-reductase, reducing the Fe-O_2 adducts to give a short-lived peroxy state. The peroxy group formed in the previous step is rapidly protonated twice, releasing one molecule of H_2O . Depending on the

substrate and enzyme involved, P450 enzymes can catalyze a wide variety of reactions. After the product has been released from the active site, the enzyme returns to its original state, with a H₂O molecule returning to occupy the distal coordination position of the iron nucleus (Guengerich, 2001). Figure 1.3 represents the catalytic cycle of cytochrome P450 enzyme.

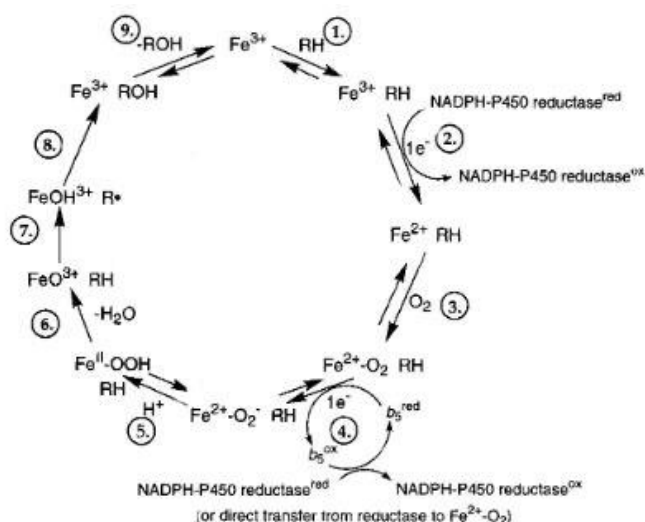


Figure 1.3 The catalytic cycle of cytochrome P450 (Guengerich, 2001).

The notable diversity of CYP enzymes has given rise to a systematic classification of individual forms into families and subfamilies. The human genome encodes 57 different CYP subfamilies in 18 families (Guengerich, 2003). The protein sequences within a given gene family are at least 40% identical, whereas the sequences within a given subfamily are more than 55% identical.

P450s are named using the symbol CYP, followed by an Arabic numeral designating the family number, a letter denoting the subfamily, and another Arabic numeral representing the individual gene (Nebert *et al.*, 1987). For example; CYP2E1 is the cytochrome P450 in family 2, subfamily E, and

gene product 1 in the subfamily. Table 1.2 represents the CYP families in human.

Table 1.2 CYP families and functions in human (Nelson, 2009).

CYP FAMILIES	NAMES	FUNCTION
CYP1	1A1, 1A2, 1B1	Xenobiotic metabolism
CYP2	2A6, 2A7, 2A13, 2B6, 2C8, 2C9, 2C18, 2C19, 2D6, 2E1, 2F1, 2J2, 2R1, 2S1, 2U1, 2W1	Xenobiotic and steroid metabolism
CYP3	3A4, 3A5, 3A7, 3A43	Xenobiotic and steroid metabolism
CYP4	4A11, 4A22, 4B1, 4F2, 4F3, 4F8, 4F11, 4F12, 4F22, 4V2, 4X1, 4Z1	Fatty acid metabolism
CYP5	5A1	Thromboxane A ₂ synthesis
CYP7	7A1, 7B1	Bile acid biosynthesis
CYP8	8A1, 8B1	Prostacyclin synthesis and bile acid biosynthesis
CYP11	11A1, 11B1, 11B2	Steroid biosynthesis
CYP17	17A1	Estrogen and testosterone biosynthesis
CYP19	19A1	Estrogen hormone biosynthesis
CYP20	20A1	Drug metabolism and cholesterol biosynthesis
CYP21	21A2	Steroid biosynthesis
CYP24	24A1	Vitamin D degradation
CYP26	26A1, 26B1, 26C1	Retinoic acid metabolism
CYP27	27A1, 27B1, 27C1	Bile acid biosynthesis and vitamin D ₃ activation
CYP39	39A1	Cholesterol biosynthesis
CYP46	46A1	Cholesterol biosynthesis
CYP51	51A1	Cholesterol biosynthesis

1.2.1.1.1 CYP1A1

The CYP1A1 (P1-450) gene, also known as AHH (aryl hydrocarbon hydroxylase), located at 15q22- q24, composed of seven exons and six introns and contains 5810 base pairs (Nebert et al., 1985; Kawajiri et al. 1986). Human CYP1A1 (EC 1.14.14.1) is mainly found on the membrane of mitochondria and endoplasmic reticulum of extrahepatic tissues such as skin, lungs, gastrointestinal tract, and cytosol of the kidney (Nebert et al., 2004). Molecular weight of CYP1A1 is 58 kDa and its mRNA length is 2608 bp. The human CYP1A1 gene encodes 512 amino acids. The most current 3-D model was generated from the crystal structure of CYP1A1 bound to the inhibitor alpha-naphthoflavone (Walsh et al., 2013). Figure 1.4 represents 3-D crystal structure of CYP1A1.

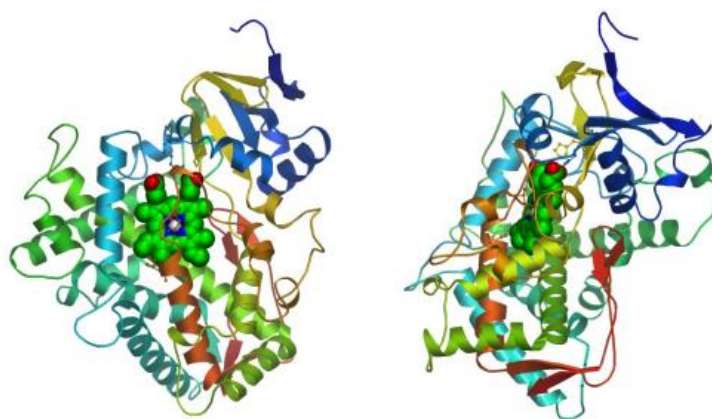


Figure 1.4 3-D crystal structure of human CYP1A1 (Walsh et al., 2013).

Studies have shown that in the absence of an inducer, only extrahepatic tissues may express low levels of CYP1A1. However, both hepatic and extrahepatic tissues express CYP1A1 when an inducer is present (de

Waziers et al. 1990; Ding and Kaminsky 2003; Galijatovic et al. 2004). CYP1A1 is both induced by and involved in the metabolism of halogenated aromatic hydrocarbons (HAHs) and polycyclic aromatic hydrocarbons (PAHs) (Knutson et al., 1982; Safe, 1990). Metabolism may lead to detoxification or bioactivation of the original substrates, and bioactivation may lead to the generation of toxic metabolites (Nebert et al., 2002).

CYP1A1 metabolizes several pro-carcinogens such as PAHs, HAHs, benzo[a]pyrene (B[a]P), 7,12-dimethyl benzantracene (7,12-DMBA), tobacco-related N-nitrosamines, as well as aflatoxin B1. These compounds are metabolized to electrophilic compounds that bind to and ultimately mutate DNA, therefore acting as strong carcinogens (Diamond et al. 1968; Kinoshita and Gelboin 1972; Hammons et al. 1997; Fujita and Kamataki 2001). Figure 1.5 represents metabolic activation of (A) B[a]P and (B) 7,12-DMBA to the carcinogenic metabolites.

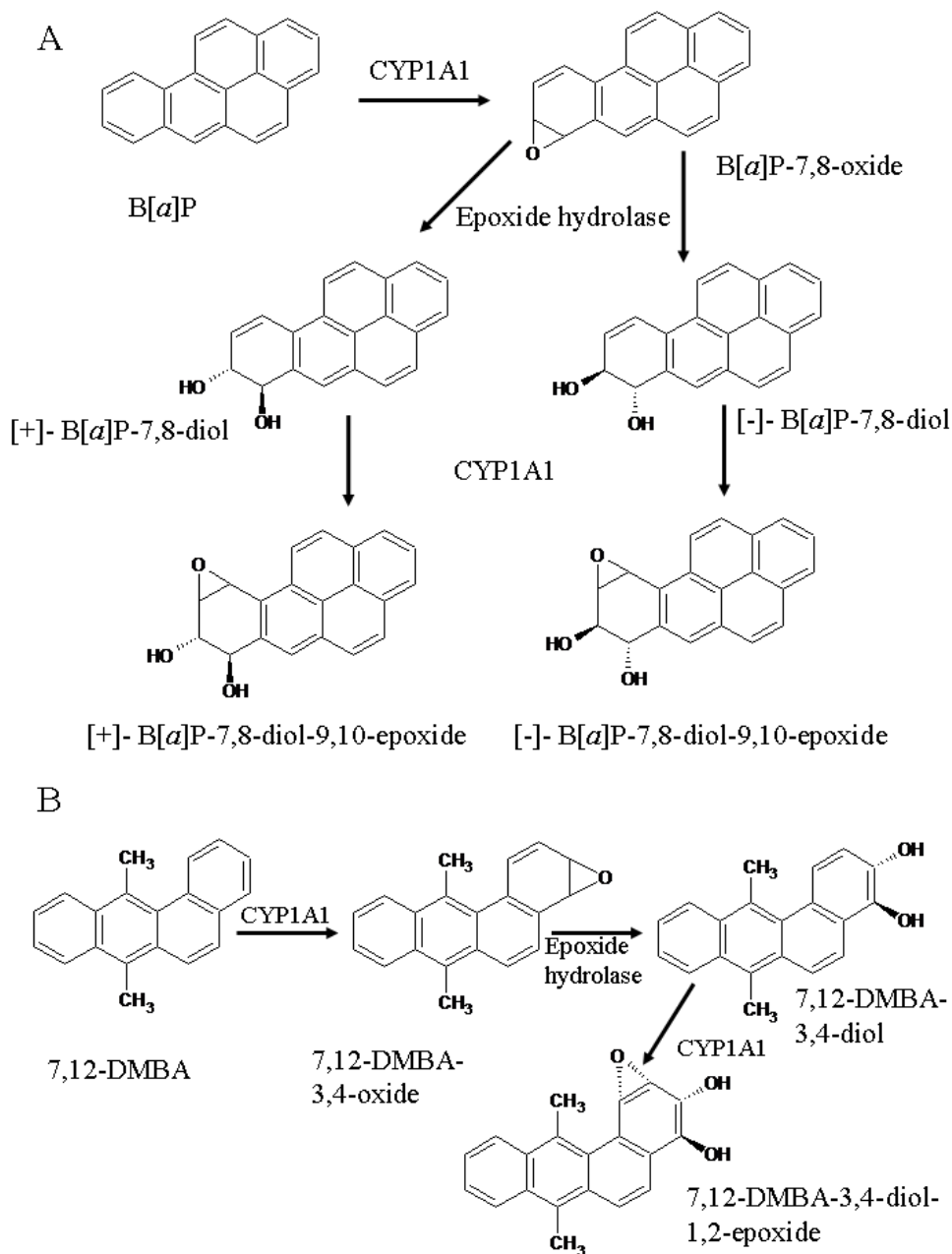


Figure 1.5 Metabolic activation of B[a]P and 7,12-DMBA to the carcinogenic metabolites (Androutsopoulos, 2009).

While formation of DNA adducts by these metabolites displays harmful effects, in the meaning of cancer this results in strong anti-cancer activity.

For example, metabolism of the pro-drug aminoflavone by CYP1A1 results in DNA adducts and they inhibit cancer growth (Hose et al. 2003; Leong et al. 2003).

Continuous exposure to airborne chemicals and environmental carcinogens is thought to increase the expression of CYP1A1 in extrahepatic tissues, through the aryl hydrocarbon receptor (AHR) (Androutsopoulos, 2009). The AHR is a soluble, ligand-activated transcription factor and member of the basic helix-loop-helix family of transcription factors (Gu et al. 2000). When in inactive form, it is located in the cytosol within a protein complex that includes two 90-kDa heat-shock proteins (HSP90), the co-chaperone p23, and a 43-kDa protein termed hepatitis B virus X-associated protein (Meyer et al. 1998). When an AHR antagonist binds to AHR, ligand-receptor complex translocate into the nucleus to form a heterodimer with ARNT. Then this heterodimer binds to promoter sequences and transcriptional cofactors to activate transcription of several genes such as CYP1A1 (Hankinson, 1995; Schmidt and Bradfield, 1996).

1.2.1.1.2 CYP2E1

Human CYP2E1 (EC 1.14.13.), the ethanol-inducible form, metabolizes and activates a significant number of substrates to more toxic products, and it is a member of cytochrome P450 monooxygenase family. It is located on the chromosome 10 and its molecular weight is 62 kDa. CYP2E1 gene encodes 493 amino acids. It comprises approximately 10% of human hepatic CYP450s, but it is not only found in the liver. It has shown to be present in the brain, lungs, gastrointestinal tract, and kidney (Raunio et al., 1995; Arınç et al., 2000a, 2000b). It metabolizes small industrial solvents, as from pyridine to other small ketones. Ethanol, benzene, pyridine and acetone are

also known as strong inducers of CYP2E1 (Arinç et al., 1991, 2000a, 2000b; Gonzalez, 2005). CYP2E1 is involved in the activation of several carcinogens and other toxic chemicals. In addition, CYP2E1 also produces free radicals causing tissue injury (Lieber, 1997).

The active site of CYP 2E1 is relatively hydrophobic and small compared to most CYP450s. It has shown that the CYP 2E1 active site has two attached voids, one which is enclosed above I helix and the other forms a channel to the protein surface. CYP 2E1 also has an access channel orientated attached to the active site opposite of I helix and extending to the surface (Porubsky, 2008). Figure 1.6 represents the active site of CYP2E1 in every angle.

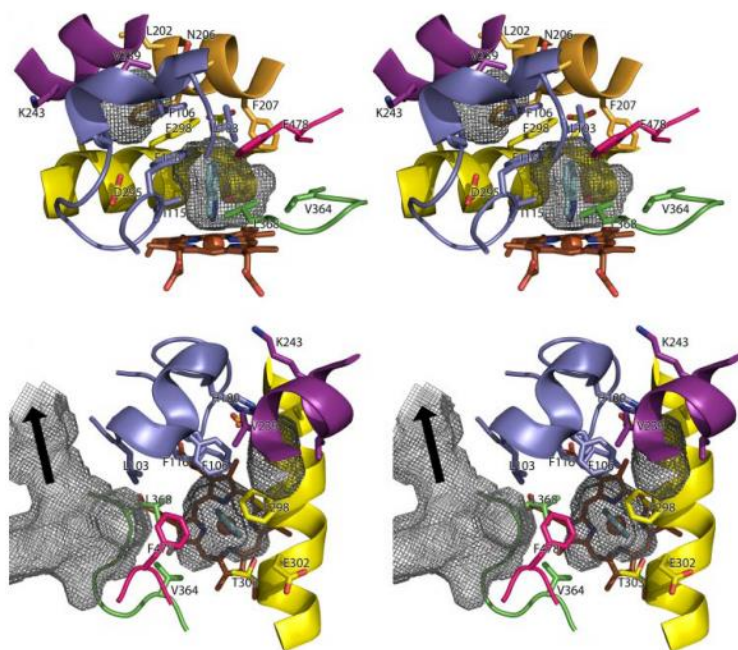


Figure 1.6 Stereo views of CYP 2E1 active site showing the ligand containing active site, small distal void, and access channel (Porubsky, 2008).

Due to the fact that CYP2E1 has a very small active site, it mostly bioactivates low molecular weight compounds such as acetaminophen, N-ethyl nitrosamine and carbon tetrachloride (Guengerich et al., 1993). It is also known that CYP2E1 is a strongly uncoupled and a highly inducible P450. Induction of CYP2E1 protein increases by alcohol, diabetes or fasting and it likely contributes to an increase in the generation of reactive oxygen species as well (Oneta et al., 2002; Arınç et al., 2005; Cederbaum et al., 2006; Arınç et al., 2007). The increase in reactive oxygen species may lead to oxidative stress. Table 1.3 represents the substrates, inducers and inhibitors of CYP2E1.

Table 1.3 Substrates, inducers and inhibitors of CYP2E1 (Modified from “Drug Interactions: Cytochrome P450 Drug Interaction Table” in by Flockhart DA, 2007).

SUBSTRATES		
ENDOGENOUS	EXOGENOUS	
	THERAPEUTIC DRUGS/ANAESTHETIC GASES	SOLVENTS AND OTHER CHEMICALS
Ethanol Acetone Acetol Acetoacetate Fatty acids (arachidonic acid, lauric acid) Glycerol	Acetaminophen Chlorzoxazone Dapsone Enflurane Halothene Disulfram Isoniazid p-nitrophenol Phenacetin	Acrylonitrile Alcohols Acetone Benzene Chloroform Styrene Carbontetrachloride Pyrazol Phenol Pyridine Acrylamide Nitrosamines Diethylether Hexane Butadiene Ethylene dibromide Methyl chloride
INDUCERS		INHIBITORS
Ethanol Acetone Benzene Isoniazid Isopropanol Pyrozol Pyridine Diabetes Starvation		Diallylsulfide Diallylsulfone Chlormethiazole Diethyldithiocarbamate Isothiocyanates 4-methyl-pyrazole Disulfram

1.2.2 Phase II Xenobiotic Metabolizing Enzymes

The main function of the phase II xenobiotic metabolizing enzymes in detoxification reactions is conjugation. These conjugation reactions are mostly catalyzed with charged species such as glutathione, sulfate, glycine, or glucuronic acid. Conjugation reactions occur on the xenobiotic sites comprising hydroxyl (-OH), amino (NH₂), sulfhydryl (-SH) and carboxyl (-COOH) groups. The purpose of these conjugation reactions is to produce more hydrophilic compounds in order to promote their excretion. Phase II enzyme family is composed of transferases including the sulfotransferases, UDP-glucuronosyltransferase, epoxide hydrolase, glutathione -S-transferases (GST), NAD(P)H quinone oxidoreductase I (NQO1), acetyl transferases and amine oxidases.

1.2.1.1 Glutathione S-Transferase

Glutathione S-transferases (GSTs) (EC.2.5.1.18) are dimeric enzymes with subunits of 199–244 amino acids in length. Molecular weight of each monomer is approximately 25 kDa. GSTs are present throughout the body but have strong activity in the liver, kidney, colon, testis, and adrenal glands (Klaassen et al., 1986). Their best known function is to catalyze the conjugation reaction of glutathione when it is in the reduced form to xenobiotic compounds in order to detoxify them. GSTs are divided into three subfamilies, which are cytosolic, mitochondrial and microsomal GSTs. Cytosolic GSTs are further divided into 8 classes assigned on the sequence similarity including Alpha, Mu, Pi, Theta, Kappa, Zeta, Omega, and Sigma.

The enzyme's highly specific active site for binding glutathione is called the G-site, while the less selective binding site for hydrophobic xenobiotics is called the H-site. Figure 1.7 represents the 3-D structure of GST enzyme.

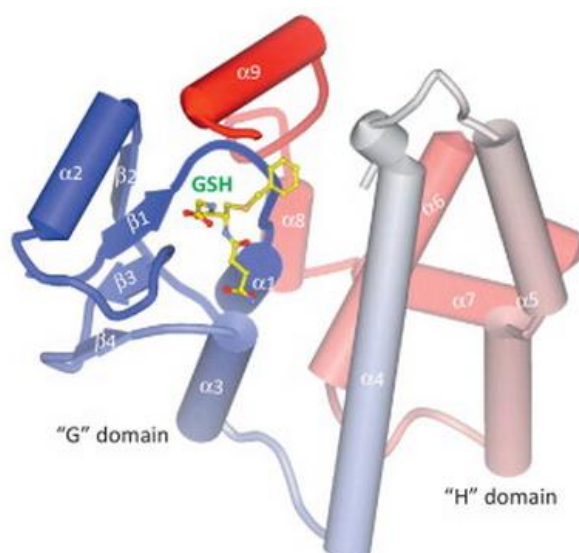


Figure 1.7 3-D structure of GST enzyme (Wu and Dong, 2012).

GSTs detoxify xenobiotic compounds by catalyzing the transfer of the glutathione thiolate on the electron deficient atom, such as sulfur, of the hydrophobic, electrophilic xenobiotic. GSTs bind both the substrate and GSH at the enzyme's hydrophobic H-site and at the hydrophilic G-site, respectively. GSTs utilize the binding cofactor tripeptide glutathione, which is composed of glycine, glutamic acid, and cysteine (Klaassen et al., 1986). Since conjugation results in the formation of a very hydrophilic metabolite, which cannot diffuse through the membrane, it is actively transported from the cell, usually by the type of transport proteins known as multi-drug resistance proteins, and is eventually transferred to the kidney. In the kidney the glutamate and glycine are cleaved and the remaining conjugate is processed further to form the final metabolite mercapturic acid, which is finally excreted in urine (Hayes et al., 1996). Figure 1.8 represents a general conjugation reaction catalyzed by GSTs.

1.2.1.2 NAD(P)H: Quinone Oxidoreductase I

NAD(P)H: Quinone Oxidoreductase I (NQO1) (EC 1.6.99.2) is a homodimeric enzyme, which belongs to the phase II enzyme family in humans and is encoded by the NQO1 gene, which is located on chromosome 16q22. Each monomer of the enzyme consists of 273 amino acids and the molecular weight of the enzyme is 31 kDa. The monomers are composed of two domains: a catalytic domain (N-terminal) (red and blue areas in Figure 1-4) 1-221, and a smaller C-terminal domain. (Yellow and Green areas) NQO1 uses FAD as a cofactor. Figure 1.9 represents the 3-D structure of NQO1 enzyme (Gad Asher, 2006).

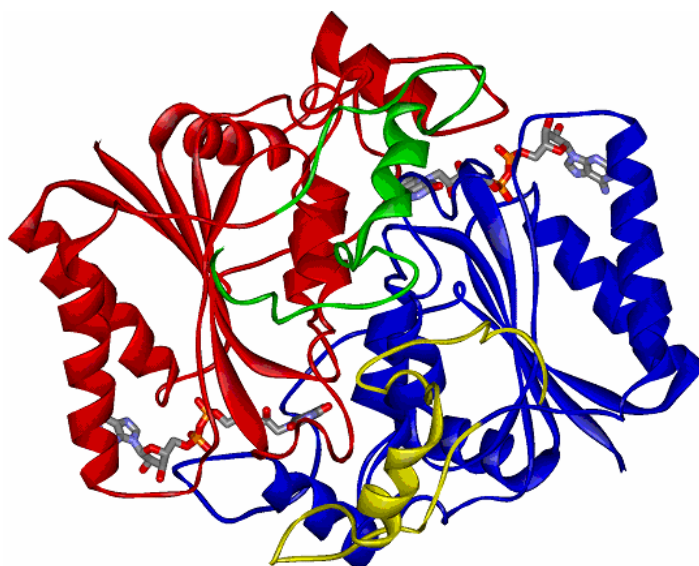


Figure 1.9 3-D structure of NQO1 enzyme. Red and blue areas represent N-terminal domain, whereas yellow and green areas represents C-terminal domain (Asher et al., 2006).

Approximately 90% of the protein is present in the cytosol of cells and it is present in various tissues including lung, breast, colon and liver. Moreover,

studies have shown that the expression of NQO1 is high in solid tumors with respect to normal tissues (Simeone et al. 2003).

The main function of the NQO1 enzyme is to perform two-electron reduction of various compounds but the most efficient substrates are quinones. It catalyzes this reduction reaction by ping-pong mechanism as given in Figure 1.10. In this mechanism of reaction, a hydride ion from NAD(P)H is transferred to the FAD then NAD(P)⁺ is released. This is the first half of the reaction. In the second half, FADH₂ donates a hydride to the quinone hydride-acceptor substrate and hydroquinone is released (Cavelier et al., 2001). Figure 1.10 represents the ping-pong mechanism used by NQO1. In addition, the two-electron reduction of quinones prevents the generation of reactive oxygen species (ROS) (Thor et al., 1982).

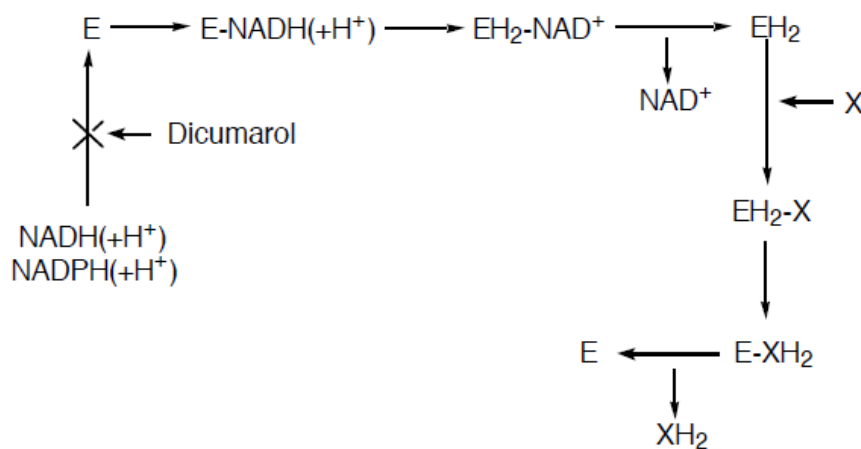


Figure 1.10 Ping-pong enzymatic mechanism of NQO1 (Ross et al., 1994).

Although the most famous substrate of NQO1 is quinones, it is known that it metabolizes several other xenobiotic including nitro-compounds such as nitrobenzamides and dinitropyrenes (Ross et al., 2000). This ability to

inactivate various reactive species makes them potent chemoprotective enzymes. Moreover, since Huggins and Fukunishi published their study in 1964, NQO1 has been recognizing as a cancer preventive enzyme as well. It is reported that increased NQO1 enzymatic activity is present in human lung, breast, colon and liver primary solid tumors with respect to the normal tissues from the same patients (Schlager et al., 1990).

NQO1 activity can be regulated by several compounds. Studies have represented that NQO1 is induced by phenolic compounds, which has been shown to have anticarcinogenic effects (Valerio et al., 2001; Çelik et al., 2014). Antioxidants, including vitamins are also shown to induce NQO1 activity (Wang and Higuchi, 1995). It is also represented that dicoumarol is a competitive inhibitor of NQO1 (Chen et al., 1999).

1.3 Aim of the Study

Vast majority of plants have been used for centuries in the treatment of various diseases, especially cancers, without knowing exactly which component have the anticarcinogenic effect through which mechanism, and this ambiguity leads scientists to investigate the effects and mechanisms of the plant phenolic compounds. Studies have shown that some of these phenolic compounds have anti-oxidative, anti-carcinogenic and anti-mutagenic effects and a small number of these compounds have more effects than the others. Quercetin is one of the best representatives for these compounds. One possible mechanism by which quercetin reduces the proliferation of cancer cells is by regulation of phase I and phase II xenobiotic metabolizing enzyme activity. *In vitro* studies conducted directly on human cells are very important to reveal these mechanisms. Moreover, in the light of these studies on the phase I and phase II enzymes, it may be

possible to improve the existing chemotherapeutic drugs or design more potent future drugs.

Since up to 80% of all colorectal cancer cases are ascribable to diet, a human colorectal cancer cell line, SW620, is a good candidate for the *in vitro* investigation of the effects of phenolic compounds on phase I and phase II xenobiotic metabolizing enzymes. For this purpose, quercetin is used as the investigated phenolic compound on human colorectal cancer cell line SW620. After proper quercetin treatments, protein and total RNA were obtained from SW620 cell culture and the protein and mRNA expressions of CYP1A1, CYP2E1, GSTP1 and NQO1enzymes were detected by Western Blot technique and qRT-PCR method, respectively.

CHAPTER 2

MATERIALS AND METHODS

2.1 Materials

2.1.1 Cell Line

In this study, protein and mRNA expressions of drug and carcinogen metabolizing enzymes CYP1A1, CYP2E1, NQO1 and GSTP1 in human colorectal adenocarcinoma cell line SW620 were analyzed. Studied cell line SW620 (ATCC® CCL-227™) was a gift from Assoc. Prof. Dr. Sreeparna Banerjee, Biology Department, Middle East Technical University.

2.1.2 Chemicals and Materials

Quercetin (Q4951), Bicinchoninic acid (D8284), ammonium acetate (A7672), bovine serum albumin (BSA; A7511), phenyl methane sulfonyl fluoride (PMSF; P7626), sodium potassium tartarate (Rochella salt; S2377), 2-amino-2(hydroxymethyl)-1,3-propanediol (Tris; T1378), acrylamide (A-8887), ammonium per sulfate (APS; A-3678), bromophenol blue (B5525), diethanolamine (D-2286), diethylpyrocarbonate (DEPC; D5758), glycerol (G5516), glycine (G-7126), β -mercaptoethanol (M6250), methanol (34885), N'-N'-bis-methylene-acrylamide (M7256), N-N-dimethylformamide (D-8654), phenazine methosulfate (P9625), secondary antibody AP rabbit (A3687), sodium dodecyl sulfate (SDS; L4390), sodium-potassium (Na-K) tartarate (S-2377), and tween 20 (P1379) were the products of Sigma Chemical Company, Saint Louis, Missouri, USA.

Magnesium chloride (MgCl_2 ; 05833), potassium chloride (KCl 104935), potassium dihydrogen phosphate (KH_2PO_4 ; 04871), di-potassium hydrogen phosphate (K_2HPO_4 ; 05101), sodium carbonate (06398), sodium hydroxide (06462), boric acid (A949265), chloroform (1.02431.2500), copper (II) sulfate pentahydrate ($\text{CuSO}_4 \cdot 5\text{H}_2\text{O}$; A894987 605), folin-phenol reagent (1.09001.0500), sodium carbonate (Na_2CO_3 ; 1.06392), sodium chloride (NaCl; 1.06400), sodium hydroxide (NaOH; 06462), zinc chloride (ZnCl_2 ; 108815) were purchased from E. Merck, Darmstadt, Germany.

Absolute ethanol (32221) and acetyl acetone (33005) were purchased from Riedel de-Haen Chemical Company, Germany. TRIzol® (15596) was obtained from Carlsbad, CA, USA. Isopropanol (AS040-L50) was the product of Atabay, Istanbul, Turkey.

5-bromo 4-chloro 3-indoyl phosphate (BCIP; R0821), dithiothreitol (DDT; R0861), gene ruler™ 50 bp DNA ladder (SM0371), light cycler-fast start DNA MasterPlus SYBR green I (K0252), Maloney murine leukemia virus reverse transcriptase (M-MuLu-RT; K1622), pre-stained protein ladder (SM0671) were the products of MBI Fermentas, USA.

Ethylene diamine tetra acetic acid (EDTA; A5097) and nitrotetrazolium blue chloride (NBT; A1243) were obtained from Applichem GmbH, Germany.

Non-fat dry milk (170-6404) and tetra methyl ethylene diamine (TEMED; 161-0801) were purchased from Bio-Rad Laboratories, Richmond, California, USA.

The CYP1A1 (sc-20772), CYP2E1 (sc-133491), GAPDH (sc-367714) and NQO1 (sc-16464) antibodies were purchased from Santa Cruz (Santa Cruz,

CA). GSTP1 (ab138491) antibody was product of the Abcam, Cambridge, United Kingdom. Primers were the products of Alpha DNA, Montreal, Canada.

Leibovitz's L-15 Medium (BE12-700F), and Fetal bovine serum (FBS; DE14-801FH) were the products of Lonza, Walkersville, MD, USA.

Pen-Strep solution (03-031-1B) and trypsin-EDTA solution (03-050-1B) was product of the Biological Industries, Beit-Haemek, Israel. RIPA buffer (9806) was purchased from Cell Signaling Technology, Beverly, MA.

2.2 Methods

2.2.1 Cell Culture

2.2.1.1 Cell Culture Conditions

SW620 cell line was cultured in Leibovitz's L-15 Medium containing 10% fetal bovine serum (FBS), 1% L-glutamine and 1% penicillin-streptomycin (Pen-Strep) solution. Cultures were incubated at 37°C with 5% carbon dioxide (CO₂) and 95% humidity in EC 160 NÜVE incubator. The cell culture studies were carried out in NÜVE MN 090 Class II Safety Cabinet. The growth medium of culture was renewed in 2-3 days for optimum growth conditions.

2.2.1.2 Cell Thawing

Before thawing the cells, 10 mL of growth medium, which is pre-warmed to 37°C, was transferred into T75 cell culture flask. Then, cryotubes were taken from the liquid nitrogen and the cells were defrosted at 37°C water bath and transferred immediately to T75 cell culture flask containing growth medium. Cells were incubated in CO₂ incubator at 37°C. Following day from the cell thawing, medium was renewed to eliminate dimethylsulfoxide (DMSO) and again placed into CO₂ incubator.

2.2.1.3 Subculturing the Cell Lines

When the cells were 80% confluent in the T75 flask, the medium was removed and cells were washed with 10 mL of 10 mM phosphate buffered saline (PBS). 1:3 split of cell lines was performed by adding 2 ml of pre-warmed trypsin to flask and placing the T75 flask in 37°C, CO₂ incubator until cells were detached and 4 mL of pre-warmed growth medium was added to the flask to inactivate the trypsin and the 2 ml of this mixture was transferred into new T75 flask. Then 10 mL of growth medium was added to new T75 flask and the culture was placed in 37°C, CO₂ incubator. This procedure was repeated in every 2-3 days.

2.2.1.4 Cell Freezing

When the cells were 80% confluent in the T75 flask, the medium was removed and cells were washed with 10 mL of PBS. 2 mL of pre-warmed trypsin was added to flask and placed in 37°C CO₂ incubator for 5 minutes. After being sure of all the cells were detached, 2 mL of pre-warmed growth medium was added to the flask to inactivate the trypsin. The cells in the flask with trypsin and growth medium were transferred into a 15 mL falcon tube and centrifuged at 400 x g for 5 minutes at room temperature. After centrifugation, supernatant was discarded and pellet was resuspended in 1 ml growth medium by pipetting. After that, the cell suspension was transferred to cryotube and 100 µL DMSO was added as cryoprotectant. Cryotube was immediately placed in the -80°C freezer and in a week it was transferred to liquid nitrogen tank for longer term storage.

2.2.1.5 IC₅₀ Determination for Quercetin

In order to determine IC₅₀ value cells were inoculated to 24 well plate in 1 mL at plating density 100.000 cells per well. After cell inoculation, the microtiter plates are incubated at 37° C, 5 % CO₂, 95 % air and 100 % relative humidity for 24 h prior to addition of quercetin. After 24 h, growth

medium was replaced with 1 mL quercetin treated medium ranging from 25 μ M to 200 μ M. Quercetin treated medium was prepared by solving quercetin in growth medium which contains 5% dimethyl sulfoxide (DMSO). Following quercetin addition, the plates are incubated for an additional 48 h at 37°C, 5 % CO₂, 95 % air, and 100 % relative humidity. After 48 h, Alamar Blue Assay was performed for cell proliferation. Alamar Blue (AB) is a blue colored, water-soluble, stable and more importantly non-toxic dye to the cells, so, it is a preferred cell viability test. In order to perform this assay, quercetin treated growth medium was discarded and cells are washed three times with 1 mL of 10 mM phosphate buffered saline (PBS). Then AB treated growth medium at a final concentration of 10% was added to the wells and plate was returned to the incubator for 2-4 h. In this 2-4 time interval plate was constantly checked for color shift. When AB is added to the cell culture, the oxidized form of the AB enters the cytosol and is converted to the reduced form by mitochondrial enzymes. This reaction is easily seen by color shift in the growth medium from blue to pink and measured by colorimetric methods. The absorbance of wells was read at 570 and 600 nm by Multiskan™ FC Microplate Photometer (Thermo Scientific).

The calculation of the percentage of AB reduction (%AB reduction) is as follows according to the manufacturer's protocol:

$$\%AB \text{ reduction} = \frac{(\epsilon_{ox\lambda_2})(A\lambda_1) - (\epsilon_{ox\lambda_1})(A\lambda_2)}{(\epsilon_{red\lambda_1})(A'\lambda_2) - (\epsilon_{red\lambda_2})(A'\lambda_1)} \times 100$$

In the formula, $\epsilon\lambda_1$ and $\epsilon\lambda_2$ are constants representing the molar extinction coefficient of AB at 570 and 600 nm, respectively, in the oxidized (ϵ_{ox}) and reduced (ϵ_{red}) forms. $A\lambda_1$ and $A\lambda_2$ represent the absorbance of test wells at 570 and 600 nm, respectively. $A'\lambda_1$ and $A'\lambda_2$ represent absorbance of negative control wells at 570 and 600 nm, respectively.

2.2.2 Protein Extraction

In order to perform protein extraction cells were seeded to 100 x 20mm tissue culture petri dishes at plating density 1.000.000 cells per petri dish. 6 petri dishes were used to culture the cells in order to triplicate the control group and the treated group. After 24 h, growth medium in the half of the dishes was replaced with growth medium, which contains 90 μ M quercetin (determined as IC_{50}), and the other half were replaced with fresh growth medium as the control group. After the treatment, the procedure is the same for both the control and the quercetin treated cells. When cells were 80% confluent, growth medium in the dishes were removed and the cells were washed three times by using cold (4 °C) PBS buffer. 1X RIPA buffer was prepared by dilution of commercially available 10X RIPA buffer (Cell Signaling Technology) with distilled water and 1mM phenylmethanesulfonyl fluoride (PMSF) was added to prevent protease activity. 400 μ L of the diluted RIPA buffer was added into the each dish for lysis of the cells. Dishes were incubated on ice for 5 minutes and the cells were scraped. The lysates of each dish were sonicated for 5 minutes and centrifuged at 14000 x g in a cold microfuge for 10 minutes. Supernatants were taken and stored at -80 °C freezer.

2.2.3 Determination of Protein Concentration

Protein concentrations of cell culture lysates were determined by the BCA (Bicinchoninic Acid) method using crystalline bovine serum albumin as a standard (P. K. Smith, 1985).

This method depends on reduction of Cu^{2+} ions with peptide bonds under alkaline conditions and chelation of two molecules of bicinchoninic acid with each Cu^+ ion, forming a purple color that absorbs light at a wavelength of 562 nm and the absorbance at this wavelength is proportional to the protein concentration.

Reagents:

Reagent A:

0.4 g of $\text{CuSO}_4 \cdot 5\text{H}_2\text{O}$ was dissolved in 10 mL dH_2O .

Reagent B:

8 g of $\text{Na}_2\text{CO}_3 \cdot \text{H}_2\text{O}$ and 1.6 g of $\text{NaKC}_4\text{H}_4\text{O}_6$ was dissolved with dH_2O and titrated with NaHCO_3 to pH 11.25 and the volume was completed to 100 mL with dH_2O . The pH of the solution was checked at the end.

Reagent C:

4 g of BCA was dissolved in 100 mL of dH_2O .

BCA Solution:

Reagent A, Reagent B and Reagent C were mixed in the same order with the ratio of 1:25:25. 23

Bovine Serum Albumin (BSA) Protein Standards:

0.02, 0.05, 0.075, 0.1, 0.15, 0.2 mg/mL

Protein Sample:

Samples were diluted 40 times

100 µL of BSA standards and samples were added into the 96 well-plate. Then 100 µL of BCA solution was added and incubated at 60°C for 15 minutes. The absorbances of samples were measured at 562 nm with Multiskan™ GO Microplate Spectrophotometer. Protein concentration was calculated according to the following equation;

$$\text{Protein Concentration (mg/ml)} = \frac{[\text{OD660nm}]}{\text{slope of standards}} \times \text{Dilution}$$

2.2.4 Determination of Protein Expression

2.2.4.1 Sodium Dodecyl Sulfate-Polyacrylamide Gel Electrophoresis

(SDS-PAGE)

Protein expression of drug and carcinogen metabolizing enzymes; CYP1A1, CYP2E1, NQO1 and GSTP1 in SW620 cell line were analyzed by Western blot method as described by Towbin et al. (1979). Before western blotting, proteins were separated by sodium dodecyl sulfate-polyacrylamide gel electrophoresis (SDS-PAGE) by using 4% stacking gel and 8.5% separating gel in a discontinuous buffer system as described by Laemmli (1970). Separating and stacking gel solutions were prepared freshly according to Table 2.1.

Table 2.1 Constituents of separating and stacking gel solutions for two gels.

Constituents	Separating Gel Solution	Stacking Gel Solution
Monomer Concentration	8.5 %	4%
Gel Solution	4250 μ L	650 μ L
dH₂O	6775 μ L	3050 μ L
Separating Buffer	3750 μ L	---
Stacking Buffer	---	1250 μ L
10% SDS	150 μ L	50 μ L
10%APS	75 μ L	25 μ L
TEMED	15 μ L	5 μ L
Total Volume	15 mL	5 mL

Reagents:

Gel Solution

14.6 g acrylamide and 0.4 g N'-N'-bis-methylene-acrylamide were dissolved separately with dH₂O then mixed and filtered through filter paper. The final volume was completed to 50 mL.

Separating Buffer (1.5 M Tris-HCl, pH 8.8)

18.15 g of tris-base was dissolved with 50 mL dH₂O, and titrated with 10 M HCl to pH 8.8. The volume was completed to 100 mL. The pH was checked at the end.

Stacking Buffer (0.5 M Tris-HCl, pH 6.8)

6 g of tris-base was dissolved with 60 mL dH₂O, and titrated with 10 M HCl to pH 6.8. The volume was completed to 100 mL. The pH was checked at the end.

Sodium Dodecyl Sulfate - SDS (10%)

1 g of SDS was dissolved with dH₂O, and the volume was completed to 10 mL.

Ammonium Persulfate - APS (10%, Fresh)

40 mg of APS was dissolved in 400 µL distilled water.

Tetramethylethylenediamine - TEMED (Commercial)

Sample Dilution Buffer-SDB (4x)

2.5 mL of 1 M tris-HCl buffer (pH 6.8), 4 mL glycerol, 0.8 g SDS, 2 mL β-mercaptoethanol and 0.001 g bromophenol blue were used and the volume was completed to 10 mL with dH₂O.

Electrophoretic Running Buffer - ERB:

0.25 M Tris, 1.92 M glycine (10x Stock, diluted to 1x before use by adding 0.1% SDS)

15 g tris-base was dissolved with 350 mL dH₂O, and then 72 g glycine was added. The volume of the mixture was completed to 500 mL.

It was prepared as 10x stock solution and it was diluted to 1x. 1 g of SDS was added per liter of 1x buffer before use.

SDS-PAGE was performed on 8.5% separating gel for CYP1A1, CYP2E1, GSTP1 and NQO1 enzymes in a discontinuous buffer system. Vertical slab gel electrophoresis was carried out using Mini-PROTEAN tetra cell mini

trans blot module (Bio-Rad, Richmond, CA). Sandwich unit of module was set up by using two glass plates with 1 cm space. Separating gel solution was prepared according to Table 2.2 and immediately the solution was transferred into the sandwich unit up to 1 cm below the comb. The top of the separating gel was covered by adding isopropanol in order to obtain smooth gel surface while providing fast polymerization of separating gel. After the polymerization of separating gel, the alcohol was removed and the stacking gel solution was poured and immediately the comb was placed. After the polymerization of stacking gel, the comb was removed. The wells were filled out with 1 x ERB and cleaned up by a syringe to remove air bubbles and remaining gel particles.

To get the 1 mg/mL concentration, the proteins were diluted with dH₂O according to the following formula;

$$V = \frac{[\text{Conc. of Protein}]}{1.333} \times 20 - 20$$

V is the volume of dH₂O to be added to dissolve 20 μL of sample.

After mixing 25 μL of 4x SDB with 75 μL of sample, the samples were incubated 1.5 minutes at 100°C heat block. Then, 20 μg of each sample was loaded on different wells. 5 μL of protein ladder was loaded as marker. After loading the samples, gel running module was placed in the main buffer tank filled with ERB. The tank was connected to the Bio-Rad power supply and electrophoresis was run at 10 mA–90 V in stacking gel and 20 mA–200 V in separating gel.

2.2.4.2 Western Blotting

Reagents:

Transfer Buffer: (25 mM Tris, 192 mM Glycine)

3.03 g trisma-base and 14.4 g glycine was dissolved in 200 mL methanol, and the volume was completed to 1 L with distilled water.

TBST: (20 mM Tris-HCl pH 7.4, 500 mM NaCl, 0.05% Tween 20)

9.5 g of NaCl was dissolved in some water and 6.5 mL of 1 M tris-HCl buffer was added. Then pH of the solution was adjusted to 7.4. Finally, 165 μ L tween 20 was added and volume was completed to 350 mL with distilled water.

Blocking Solution: (5% Non-Fat Dry Milk)

5 g non-fat dry milk was dissolved in 100 mL TBS

Primary Antibody: 1/200 to 1/1000 dilutions

Secondary Antibody: 1/500 to 1/5000 dilutions

Alkaline Phosphatase Substrate Solution:

Solution A: 2.67 mL of 1.5 M Tris-HCl Buffer (pH 8.8), 4 mL of 1 M NaCl, 96 μ L of Diethanolamine, 820 μ L of 100 mM $MgCl_2$, 40 μ L of 100 mM $ZnCl_2$ and 12.2 mg of Nitrotetrazolium Blue Chloride (NBT) were mixed and the pH of the mixture was adjusted to 9.55 with saturated Tris. Then the volume was completed to 40 mL with distilled water.

Solution B: 2 mg of Phenazine Methosulfate was dissolved in 1 mL of distilled water.

Solution C: 5.44 mg of BCIP (5-bromo 4-chloro 3-indoyl phosphate) was dissolved in 136 μ L of N-N-dimethylformamide.

To prepare the substrate solution, 20 mL of Solution A, 68 μ L of Solution C, and 134 μ L of Solution B were mixed for each membrane.

HRP-ECL Substrate Solution: (Pierce ECL Western Blotting Substrate)

1 mL of Peroxide solution and 1 mL of luminol enhancer solution were mixed and 2 mL of this mixture was used for each membrane.

For western blotting, the gel was removed from the glasses and the gel was placed into transfer buffer for 10 minutes. The PVDF membrane was cut as equal size with the gel and immersed in 100% methanol for a few seconds to pre-wet the membrane. Then the membrane was equilibrated in transfer buffer for 5 minutes. After that, the gel, PVDF membrane, Whatman papers and two fiber pads were placed in transfer sandwich as shown in Figure 2.1. The transfer sandwich was placed into Mini Trans-Blot module (Bio-Rad Laboratories, Richmond, CA, USA) and module was filled with transfer buffer. The transfer was carried out at 90 volt and 400 mA for 90 minutes.

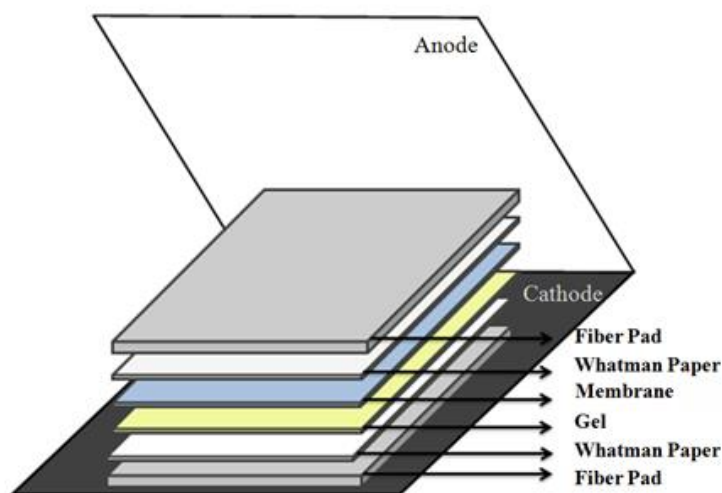


Figure 2.1 Western blot sandwich

After transfer was completed, the membrane was washed with TBST for 10 minutes. Then membrane was incubated with blocking solution in room temperature for an hour. After that, the membrane was incubated with 1/500 dilutions of CYP1A1, CYP2E1 and NQO1 while 1/1000 dilution of GSTP1

primary antibodies for 2 h at room temperature by shaking. The membrane was washed with TBST for three times each of which is 10 minutes. After removal of unbound primary antibody, the membrane was incubated with 1/2000 dilutions of alkaline phosphatase conjugated secondary antibodies for CYP1A1 and CYP2E1; and 1/4000 dilutions of horseradish peroxidase (HRP) conjugated secondary antibodies for NQO1 and GSTP1 for an hour. Finally the membrane was incubated with suitable substrate solution for the conjugated enzyme on the secondary antibody. For visualization of HRP conjugated secondary antibody, X-Ray Roentgen Method was used and the bands were visualized on the roentgen film. The band intensities were analyzed by Image J visualization software developed by NIH.

2.2.5 Determination of mRNA Expression

2.2.5.1 Isolation of Total RNA from Cell Lines

All plastic and glass equipments used for total RNA isolation were treated with distilled water containing % 0.1 (v/v) diethylpyrocarbonate (DEPC) in order to inhibit RNase activity. After the evaporation of excess DEPC, the equipment was autoclaved.

Cell lines were seeded into 12 well plate for RNA isolation. After 24 h growth medium in the half of the wells were replaced by quercetin treated growth medium, whereas the other half was replaced with fresh growth medium. When cells were 80% confluent, growth medium in the wells was removed and the cells were washed three times by using PBS buffer. After that, 1 mL of Trizol®, was added into the wells and incubated for 5 minutes at room temperature. After incubation, the cells were detached by pipetting and Trizol® solution containing the cell lysate in the well was transferred into a 2 mL eppendorf tube. 200 µL of chloroform was added to tube and the tube was shaken vigorously. The tube was centrifuged at 12000 x g for 15 minutes at 4°C which produce three layers. The upper aqueous phase

containing RNA was taken and same amount of cold isopropanol was added into the tube and the tube was shaken gently. The mixture was incubated at room temperature for 10 minutes. Then, it was centrifuged at 12000 x g for 20 minutes at 4°C. The supernatant was removed and the pellet was mixed with 1 mL of 75% ethanol. The tube was centrifuged again at 7500 x g for 5 minutes at 4°C; the pellet was taken and excess amount of ethanol was evaporated in hood. Finally, RNA was dissolved in 25 µL of nuclease-free distilled water and stored at -80°C.

2.2.5.2 Determination of RNA Concentration

Concentration of the isolated RNA was quantified by measuring the absorbance at 260 nm. Purity was assessed by the 260/280 nm ratio. The ratio of OD₂₆₀/OD₂₈₀ must be between 1.8 and 2.2. Below 1.8 refers the DNA contamination while above 2.2 referring the protein contamination. The optical density of 1.0 corresponded to the 40 µg/mL for RNA. The concentration and purity of the RNA were measured at NanoDrop™ 2000 (Thermo Scientific).

2.2.5.3 Qualification of RNA Molecules by Agarose Gel Electrophoresis

Presence and the purity of RNA were checked on 1% (w/v) agarose gel by using horizontal agarose gel electrophoresis unit. 1% (w/v) agarose was prepared by mixing 1 g of agarose with 100 ml 0.5 X Tris –Borate-EDTA (TBE) buffer, pH 8.3. The agarose was dissolved in a microwave oven. The solution was cooled approximately 60°C. 7 µL of ethidium bromide solution (10 mg/mL) was added and the solution was mixed thoroughly. Agarose gel solution was poured into electrophoresis tray and the comb was placed for well formation. After the gel polymerization, gel tank was filled with 0.5 X TBE buffer. The comb was removed. 5 µL of RNA solution was mixed with 1 µL of 6 X loading dye and the mixture was loaded into wells.

Electrophoresis was performed at 90 mV for 1 hour. The gel was observed and photographed under UV light.

2.2.5.4 cDNA Synthesis

Reagents:

5X Reaction Buffer : 250 mM Tris-HCl pH 8.3, 250 mM KCl, 20 mM MgCl₂ and 50 mM DDT

M-MuLV-RT: Moloney-Murine Leukemia Virus Reverse Transcriptase

Ribolock: RNase inhibitor

dNTP: Deoxyribonucleotide triphosphate (10mM)

Reverse transcription of RNA to cDNA was performed by mixing 1 µg of total RNA isolated from cell lines and 1 µL of oligo dT primer (Fermentas, Hanover, MD, USA) in an eppendorf tube. The final volume of the mixture was completed to 12 µL with nuclease-free distilled water. The solution was mixed gently and spinned down by microfuge. Mixture was incubated at 70°C for 5 minutes and it was chilled on ice. After that, 4 µL of 5X reaction buffer, 1 µL Ribolock and 2 µL of 10 mM dNTP were added. The tube was mixed gently and spinned down by microfuge. It was incubated at 37°C for 1 hour. Finally, the reaction was stopped by keeping at 70°C for 10 minutes and chilled on ice. cDNA was stored at -20°C for further use.

2.2.5.5 Quantitative Real-Time PCR

The expressions of CYP1A1, CYP2E1, NQO1 and GST genes in cell lines were analyzed by quantitative Real Time PCR (qRT-PCR) using Corbett Rotor Gene 6000 (Corbett life Science, PO Box 435, Concorde, NSW 2137). The 25 µL of final reaction mixture containing 100 ng cDNA, 0.5

mM reverse and forward primers and 1 X Maxima® SYBR Green qPCR Master Mix (Fermentas, Glen, Burnie, MD) and RNase free distilled water. In order to detect any contamination, no template control (NTC) was used. As an internal standard, GAPDH (glyceraldehyde 3-phosphate dehydrogenase) gene was used. The DNA amplification was carried out in a reaction mixture containing specific nucleotide sequence for related gene is given in Table 2.3. The qRT-PCR program consisted of the following cycling profile; initial melting at 95 °C for 10 minutes, amplification and quantification program repeated 45 times containing melting at 95 °C for 20 seconds, annealing at 58-60 °C (depending on the gene) for 20 seconds and extension at 72 °C for 20 seconds with a single fluorescent measurement. After cycling, melting curve program 50-99 °C with a heating rate of 0.1 °C/s and continuous fluorescence measurement was added. Melting curve analysis of the amplification product was done at the end of each amplification reaction to confirm the detection of a PCR product. Quantities of specific mRNAs in the sample were measured according to corresponding gene and relative standard curve method. In each assay, a standard curve was calculated concurrently with the control and the quercetin treated cells. Each Standard curve was derived from dilution series (1:10, 1:100, 1:500, 1:1000, 1:5000) of selected standard cDNA for each gene. Light cycler quantification software was used to draw the standard curve.

Table 2.2 Primer sequences, annealing temperatures and product sizes of the genes.

Gene	Forward Primer (5' → 3')	Reverse Primer (5' → 3')	Annealing Temperature (°C)	Product Size (bp)
GAPDH	GAGGAGATCCCTCCAAA T	GGCTGTTGTCATACTCTCAT GG	58	197
CYP1A1	TACCTCAGCAGCCACCTCCA AG	GGCCCTGATTACCCAGAATA CC	60	121
CYP2E1	AGCGCTGCTGGACTACAAG G	CCTCTGGATCCGGCTCTCAT	60	184
NQO1	AAGAGCACTGATCGTACTG GC	GGATACTGAAAGTTCGCAGG GG	60	196
GSTP1	CCTACACCGTGGTCTATTTC C	CAGGAGGCTTTGAGTGAGC	60	137

2.2.6 Statistical Analysis

Statistical analyses were performed by using GraphPad Prism version 6 statistical software package for Windows. All results were expressed as means with their Standard Deviation (SD). Unpaired, two-tailed student's t-test and $p < 0.05$ were chosen as the level for significance.

CHAPTER 3

RESULTS

3.1 Cell Culture

3.1.1 IC₅₀ Determination for Quercetin

In this study the effects of the plant phenolic compound quercetin were studied on human colorectal cancer cell line SW620. In order to perform that, cells were inoculated to 24 well plate in 1 mL at plating density of 100.000 cells per well and incubated at 37° C, 5 % CO₂, 95 % air and 100 % relative humidity for 24 h prior to addition of quercetin. After 24 h, growth medium was replaced with 1 mL quercetin treated medium. After 48 h, Alamar Blue (AB) Assay was performed for cell proliferation as described previously in methods section. Figure 3.1 represents the color shift after AB assay.



Figure 3.1 Color shift among wells after AB assay following quercetin treatment ranging from 25 μ M to 200 μ M.

When color shift was visible from pink to blue, samples were transferred to a 96 well plate and absorbance values were read by Microplate Photometer at 570 and 600 nm. Percent reductions were calculated by following formula:

$$\%AB \text{ reduction} = \frac{(\varepsilon_{\text{ox}\lambda_2})(A\lambda_1) - (\varepsilon_{\text{ox}\lambda_1})(A\lambda_2)}{(\varepsilon_{\text{red}\lambda_1})(A'\lambda_2) - (\varepsilon_{\text{red}\lambda_2})(A'\lambda_1)} \times 100$$

Table 3.1 represents the percent AB reduction and percent survival values following the quercetin treatment ranging from 25 to 200 μM .

Table 3.1 Percent AB reduction and percent survival values of the cells following quercetin treatment ranging from 25 to 200 μM .

Quercetin Conc. (μM)	Percent Reduction	Percent Survival
0	88,21	100
25	79,90	90,57
50	62,30	70,63
75	47,93	54,33
100	33,99	38,53
125	27,98	31,72
150	25,89	29,35
175	29,29	33,21
200	29,44	33,38

According to the values, which are represented in Table 3.1, a cell proliferation graph was drawn and the equation of this graph was used in the IC50 value calculation. According to the calculations IC50 value for quercetin was determined as 90 μM . Figure 3.2 and Figure 3.3 represent the cell proliferation and percent survival graphs for quercetin treated cells, respectively.

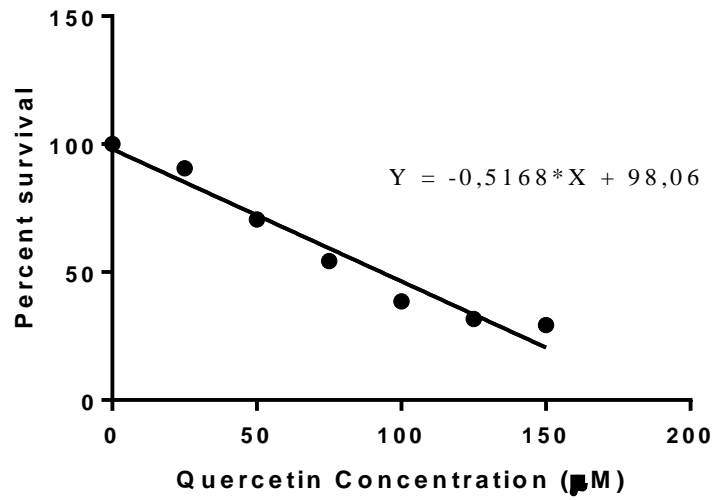


Figure 3.2 Cell proliferation graph for quercetin treated cells.

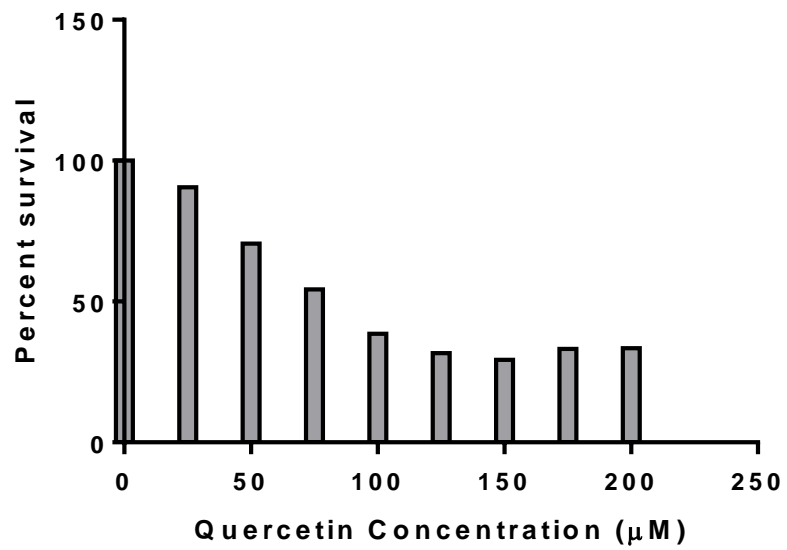


Figure 3.3 Percent survival graph for quercetin treated cells.

3.2. Protein Concentrations of Lysates of the Control and the Treated Cells

In this study the effects of plant phenolic compound quercetin on protein expressions of xenobiotic metabolizing enzymes; CYP1A1, CYP2E1, NQO1 and GSTP1 were carried out by using SW620 colon carcinoma cell line. In order to perform that, protein extraction from three replicate plates of control and quercetin treated cells was carried out by using RIPA buffer procedure and then protein concentrations were determined by BCA method as described previously in methods section. Figure 3.4 represents the control and treated plates prior to the protein extraction and average protein concentrations of control and quercetin treated cells are listed in Table 3.2.

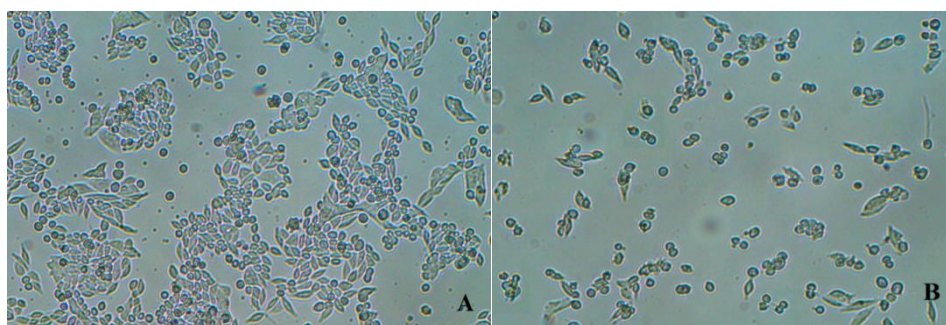


Figure 3.4 Control (A) and 90 μM (IC₅₀ value) quercetin treated (B) wells prior to protein extraction.

Table 3.2 Average protein concentrations of whole cell lysates of control and treated cells.

Cells	Average Protein Concentration (mg/mL)
Control	4.90 ± 0.02
Treated	1.12 ± 0.15

3.3 Protein Expression Analysis of CYP1A1, CYP2E1, NQO1 and GSTP1 Enzymes in SW620 Cells

Xenobiotic metabolizing phase I enzymes; CYP1A1 and CYP2E1, phase II enzymes; NQO1 and GSTP1 protein expressions in SW620 colon carcinoma cell line were determined by Western blotting. Western blot experiments were carried out on total cellular extracts of the control and treated cells. Immunochemical detection was performed by appropriate specific antibodies. GAPDH (37 kDa) was used as internal standard.

3.3.1 CYP1A1 Protein Expression in the Control and the Quercetin Treated Cells

CYP1A1 protein expression was determined by Western blotting. In order to perform immunochemical detection of CYP1A1 protein, primary rabbit polyclonal anti-CYP1A1 antibody (1/500 dilution) and an alkaline phosphatase (AP) conjugated secondary goat anti-rabbit antibody (1/2000 dilution) were used. The results of CYP1A1 protein expression in control and quercetin treated SW620 colon carcinoma cell line were shown in Figure 3.5. Band intensities were quantified by using Image J visualization software. Unpaired t-test was used to perform comparison analysis of protein expression of the control and treated cells and the level of significance was chosen as $p < 0.05$. Statistical results are shown in Figure 3.6.

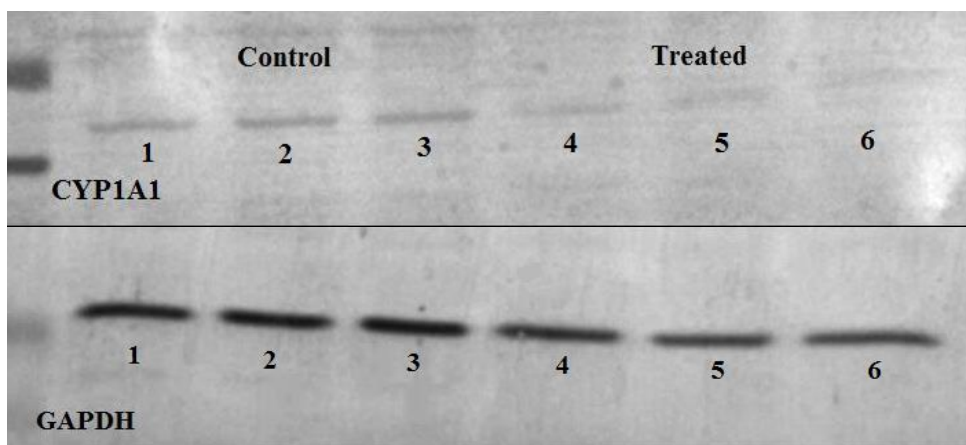


Figure 3.5 Immunoreactive protein bands of control and quercetin treated SW620 cells representing the expression of CYP1A1 (58 kDa). GAPDH (37 kDa) used as internal standard. Lane 1-3: Control, Lane 4-6: Quercetin Treated Cells. Each well is loaded with 20 μg protein.

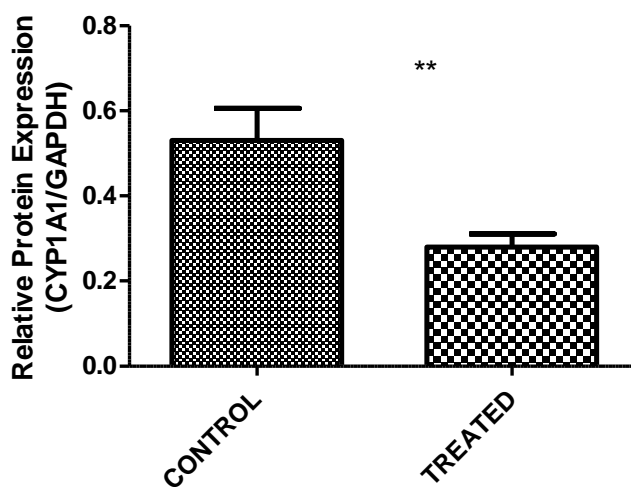


Figure 3.6 Comparison of CYP1A1 protein expression of control and quercetin treated cells. The band quantifications are expressed as mean \pm SD and experiments were carried out in triplicate. Statistical analysis of CYP1A1 protein expression was done by unpaired, two-tailed student's t-test and ** means $P \leq 0.01$.

3.3.2 CYP2E1 Protein Expression in the Control and the Quercetin Treated Cells

CYP2E1 protein expression was determined by Western blotting. In order to perform immunochemical detection of CYP2E1 protein, primary rabbit polyclonal anti-CYP2E1 antibody (1/500 dilution) and an alkaline phosphatase (AP) conjugated secondary goat anti-rabbit antibody (1/2000 dilution) were used. The results of CYP2E1 protein expression in control and quercetin treated SW620 colon carcinoma cell line were shown in Figure 3.6. Band intensity quantifications were performed by using Image J visualization software. Figure 3.7 represents the relative protein expressions between control and treated cells. Unpaired t-test was used to perform comparison analysis of protein expression of the control and treated cells and the level of significance was chosen as $p < 0.05$. Statistical results are shown in Figure 3.8.

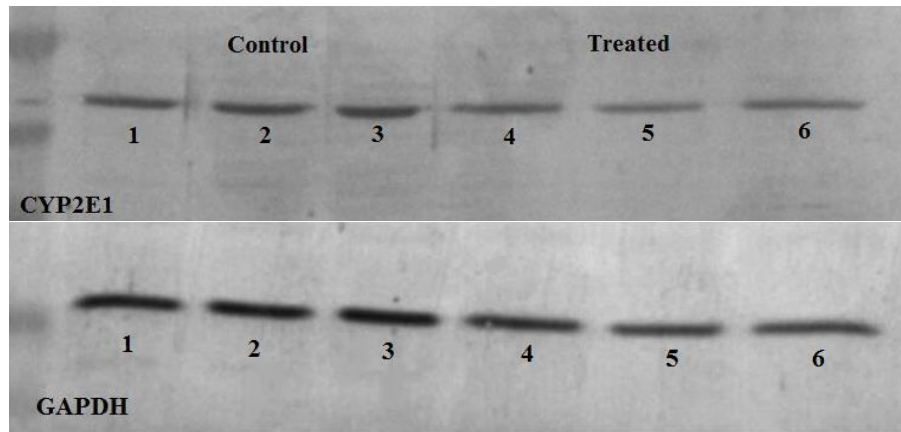


Figure 3.7 Immunoreactive protein bands of control and quercetin treated SW620 cells representing the expression of CYP2E1 (52 kDa). GAPDH (37 kDa) used as internal standard. Lane 1-3: Control, Lane 4-6: Quercetin Treated Cells. Each well is loaded with 20 μg protein.

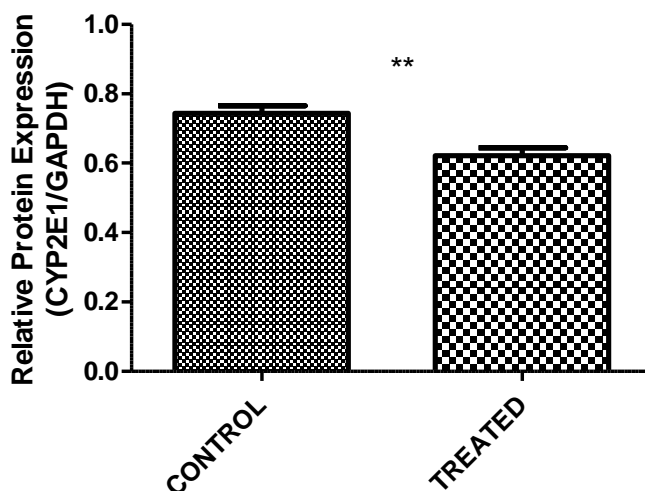


Figure 3.8 Comparison of CYP2E1 protein expression of control and quercetin treated cells. The band quantifications are expressed as mean \pm SD and experiments were carried out in triplicate. Statistical analysis of CYP2E1 protein expression was done by unpaired, two-tailed student's t-test and ** means $P \leq 0.01$.

3.3.3 GSTP1 Protein Expression in the Control and the Quercetin Treated Cells

GSTP1 protein expression was determined by Western blotting technique. In order to perform immunochemical detection of GSTP1 protein, primary goat polyclonal anti- GSTP1 antibody (1/1000 dilution) and a horseradish peroxidase (HRP) conjugated secondary mouse anti-goat antibody (1/4000 dilution) were used. The results of GSTP1 protein expression in control and quercetin treated SW620 colon carcinoma cell line were shown in Figure 3.9. Band intensity quantifications were performed by using Image J visualization software. Figure 3.6 represents the relative protein expressions between control and treated cells. Unpaired t-test was used to perform comparison analysis of protein expression of the control and treated cells

and the level of significance was chosen as $p < 0.05$. Statistical results are shown in Figure 3.10.

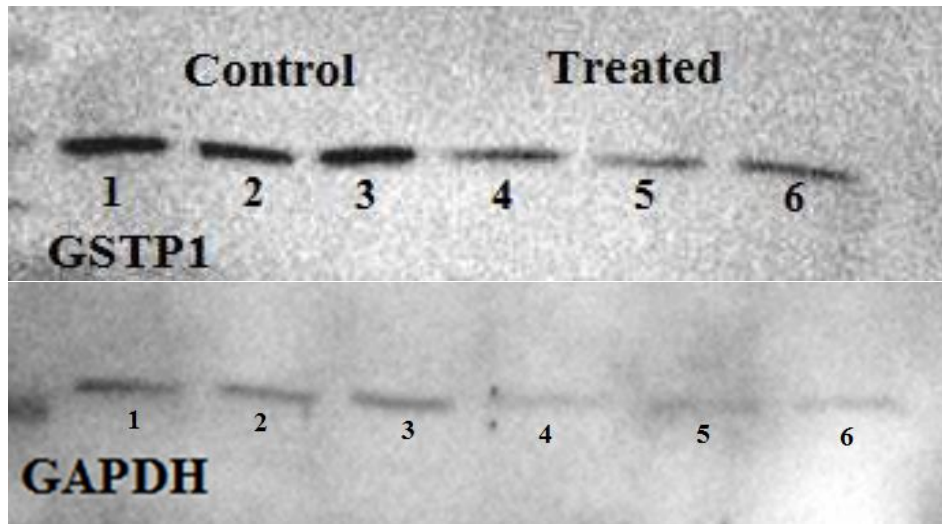


Figure 3.9 Immunoreactive protein bands of control and quercetin treated SW620 cells representing the expression of GSTP1 (23 kDa). GAPDH (37 kDa) used as internal standard. Lane 1-3: Control, Lane 4-6: Quercetin Treated Cells. Each well is loaded with 20 μg protein.

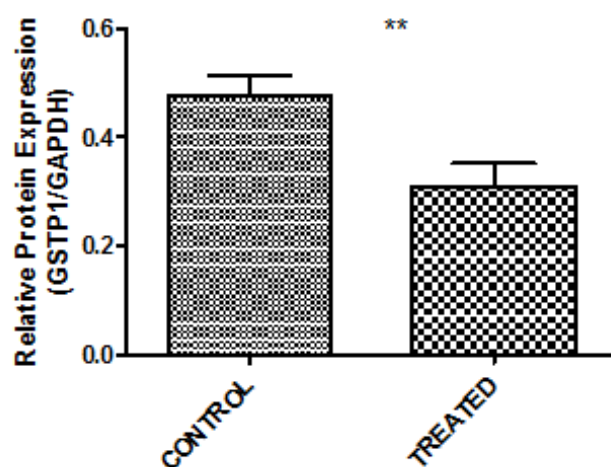


Figure 3.10 Comparison of GSTP1 protein expression of control and quercetin treated cells. The band quantifications are expressed as mean \pm SD and experiments were carried out in triplicate. Statistical analysis of GSTP1 protein expression was done by unpaired, two-tailed student's t-test and ** means $P \leq 0.01$.

3.3.4 NQO1 Protein Expression in the Control and the Quercetin Treated Cells

NQO1 protein expression was determined by Western blotting technique. In order to perform immunochemical detection of NQO1 protein, primary goat polyclonal anti-NQO1 antibody (1/500 dilution) and a horseradish peroxidase (HRP) conjugated secondary mouse anti-goat antibody (1/4000 dilution) were used. The results of GSTP1 protein expression in control and quercetin treated SW620 colon carcinoma cell line were shown in Figure 3.11. Band intensity quantifications were performed by using Image J visualization software. Figure 3.6 represents the relative protein expressions between control and treated cells. Unpaired t-test was used to perform

comparison analysis of protein expression of the control and treated cells and the level of significance was chosen as $p < 0.05$. Statistical results are shown in Figure 3.12.

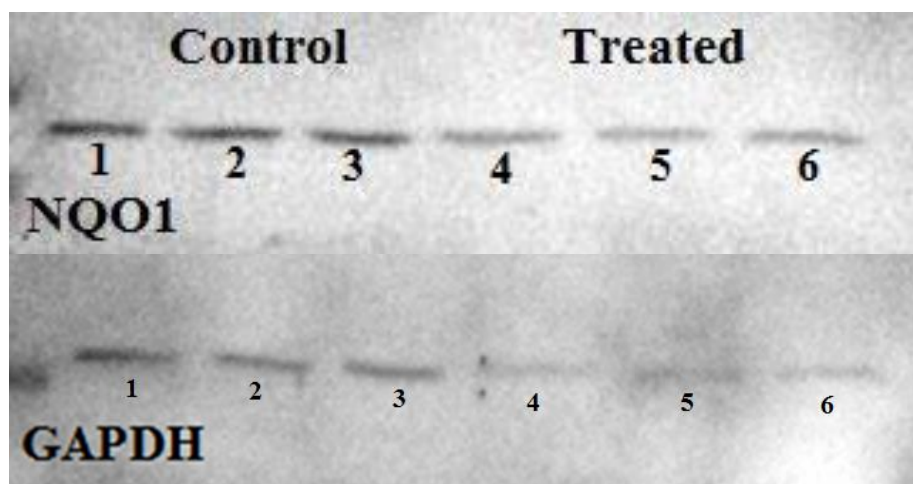


Figure 3.11 Immunoreactive protein bands of control and quercetin treated SW620 cells representing the expression of NQO1 (31 kDa). GAPDH (37 kDa) used as internal standard. Lane 1-3: Control, Lane 4-6: Quercetin Treated Cells. Each well is loaded with 20 μg protein.

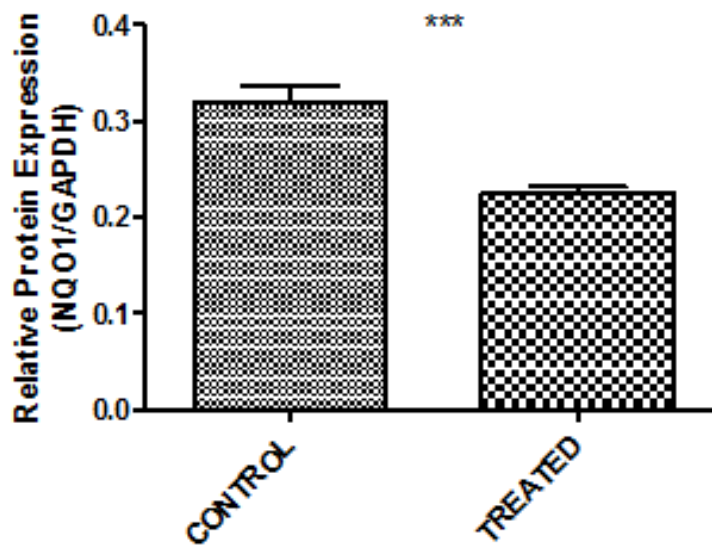


Figure 3.12 Comparison of NQO1 protein expression of control and quercetin treated cells. The band quantifications are expressed as mean \pm SD and experiments were carried out in triplicate. Statistical analysis of NQO1 protein expression was done by unpaired, two-tailed student's t-test and *** means $P \leq 0.001$.

3.4 CYP1A1, CYP2E1, NQO1 and GSTP1 mRNA Expressions in the Control and Quercetin Treated SW620 Cells

3.4.1 Quality Control of RNA Molecules by Agarose Gel Electrophoresis

Total RNA was isolated from cell lines by using Trizol[®] as described in the method section. Quantity of isolated RNA was measured by reading the absorbance at 260nm. Purity of RNA molecules were checked by NanoDrop with OD_{260}/OD_{280} and OD_{260}/OD_{230} ratios which should be in the range of 1.8-2.2 and 2.0-2.2, respectively. OD_{260}/OD_{280} ratio was used to check DNA contamination while OD_{260}/OD_{230} ratio was used to check carbohydrate and phenolic contamination. After these measurements, 28S

and 18S ribosomal RNA bands were controlled with agarose gel electrophoresis and they were well separated 28S and 18S ribosomal RNA bands on the gel (Figure 3.13).

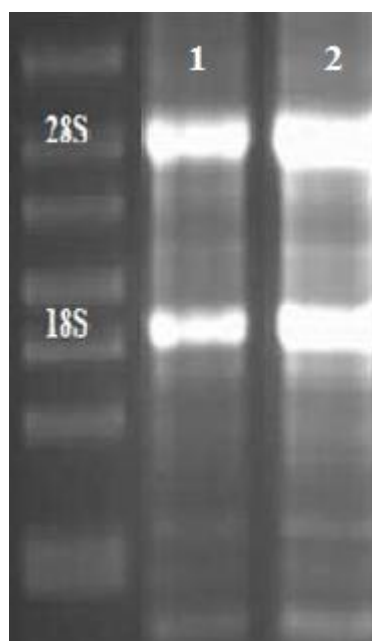


Figure 3.13 Agarose gel electrophoresis results of RNA samples isolated from quercetin treated (Lane 1) and control (Lane 2) cells. 10 μ l RNA samples were loaded in each well.

3.4.2 CYP1A1 mRNA Expression in the Control and the Quercetin Treated SW620 Cells

CYP1A1 mRNA expression was determined by quantitative real time PCR (qRT-PCR) technique and GAPDH was used as internal standard to calculate relative mRNA expression of CYP1A1. Specific annealing temperatures of the primers of CYP1A1 and GAPDH given previously in Table 2.2 were used in qRT-PCR.

Figure 3.14 shows the standard curve which was generated from 1:10, 1:100, 1:500, 1:1000, and 1:5000 diluted cDNAs of the control cells used for mRNA quantifications of the samples. Figure 3.15 illustrates the amplification plot that shows the changes in fluorescence of SYBR green dye I versus cycle number of CYP1A1 gene of control and quercetin treated cells. In Figure 3.16, melting curve with one peak is represented for the detection of single PCR product.

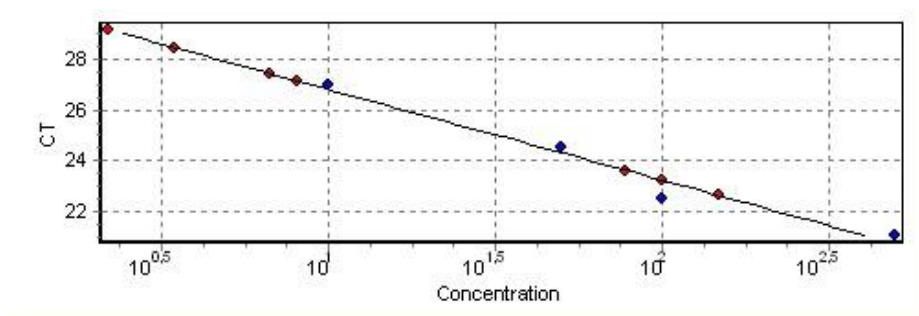


Figure 3.14 Standard curve generated from serial dilutions of control cDNA to calculate quantities of CYP1A1 mRNAs in the control and quercetin treated cells relatively.

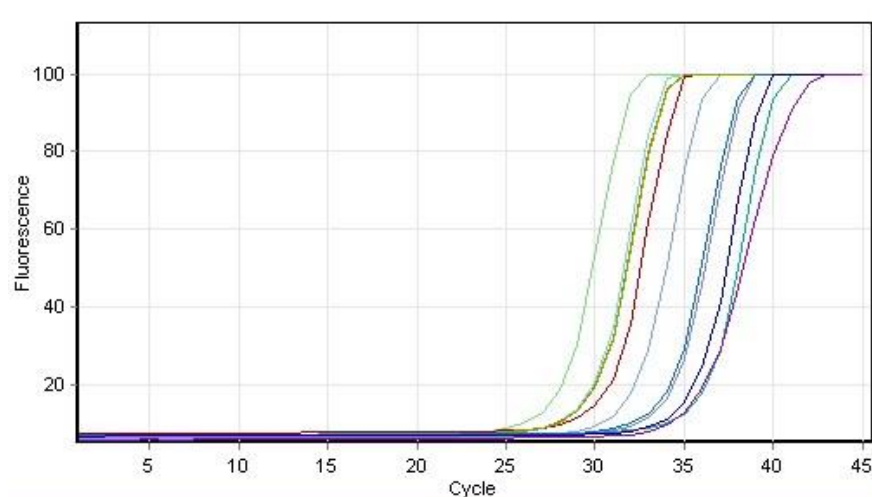


Figure 3.15 Amplification curve showing the accumulation of fluorescence emission at each reaction cycle.

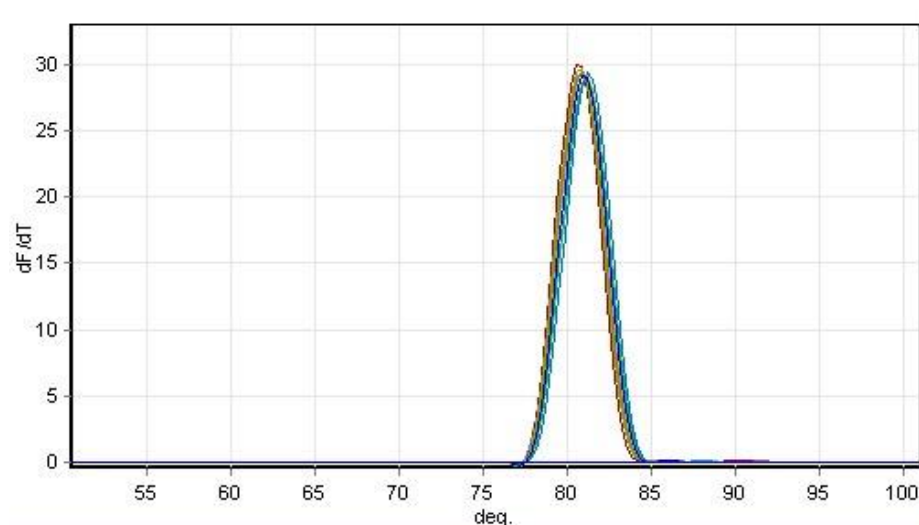


Figure 3.16 Melting curve showing the fluorescence emission change versus temperature. Detection of single peak means single PCR product.

The qRT-PCR products of CYP1A1 and GAPDH in control and quercetin treated SW620 colon carcinoma cells are given in Figure 3.17 and Figure 3.18 respectively. Bands' positions on the gel overlaps with expected size of the CYP1A1 and GAPDH qRT-PCR products which are 121 and 197 bp, respectively.

The results were normalized with internal standard GAPDH. Livak method (Livak, 2001) was used to determine relative CYP1A1 mRNA expression in control and quercetin treated cells by using Ct values. Formulation for Livak ($2^{-\Delta\Delta Ct}$) method is given in Table 3.3. For calculation of relative mRNA expression by using Livak method, Ct values of control group were used as reference.



Figure 3.17 qRT-PCR products of CYP1A1 cDNA (121bp) of control (Lane 3-5) and quercetin treated (Lane 6-8) cells. 5 μ L of qRT-PCR product was loaded in each well. Lane 1 shows the bp markers and NTC (Lane 2) is the no template control.



Figure 3.18 qRT-PCR products of GAPDH cDNA (197bp) of control (Lane 3-5) and quercetin treated (Lane 6-8) cells. 5 μ L of qRT-PCR product was loaded in each well. Lane 1 shows the bp markers and NTC (Lane 2) is the no template control.

Table 3.3 The Livak method for the calculation of relative mRNA expression using Ct values.

	Control	Treated
Ct_{CYP1A1}	25,53	28,47
Ct_{GAPDH}	19,14	20,79
$\Delta Ct_{\text{treated}} =$	Ct _{GAPDH}	- Ct _{CYP1A1}
$\Delta Ct_{\text{control}} =$	Ct _{GAPDH}	- Ct _{CYP1A1}
$\Delta Ct_{\text{treated}} =$	-6,39	-7,68
$\Delta\Delta Ct = \Delta Ct_{\text{control}} - \Delta Ct_{\text{treated}}$		
$\Delta\Delta Ct =$	0,00	1,29
$2^{-\Delta\Delta Ct}$	1	0,15

Figure 3.19 shows the mean \pm SD of the relative CYP1A1 mRNA expressions of control and quercetin treated cells. The data was statistically analyzed by unpaired, two-tailed student's t-test.

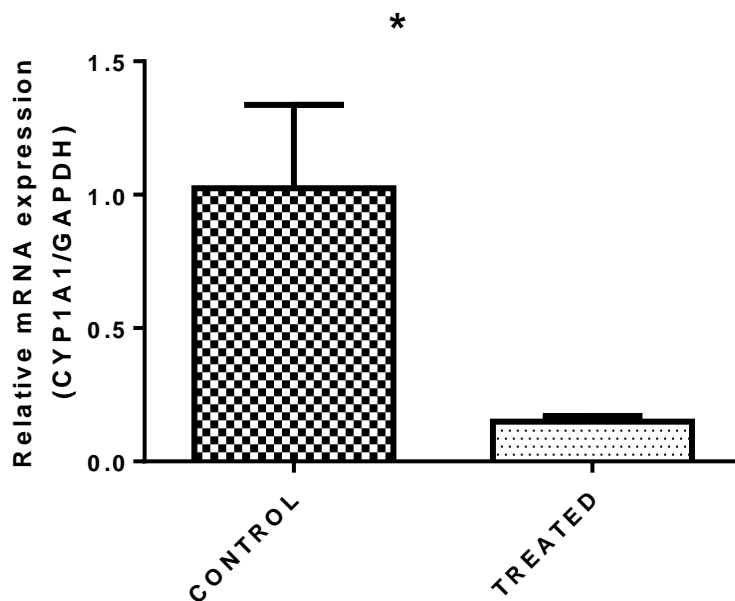


Figure 3.19 Comparison of CYP1A1 mRNA expressions between control and quercetin treated cells. The quantities are expressed as mean \pm SD of the relative expression. Experiments were carried out in triplicate. Statistical analysis of CYP1A1 mRNA expression was done by unpaired, two-tailed student's t-test. * means $p < 0.05$.

3.4.3 CYP2E1 mRNA Expression in the Control and the Quercetin Treated SW620 Cells

CYP2E1 mRNA expression was determined by quantitative real time PCR (qRT-PCR) technique and GAPDH was used as internal standard to calculate relative mRNA expression of CYP2E1. Specific annealing temperatures of the primers of CYP2E1 and GAPDH given previously in Table 2.2 were used in qRT-PCR.

Figure 3.20 shows the standard curve which was generated from 1:10, 1:100, 1:500, 1:1000, and 1:5000 diluted cDNAs of the control cells used for mRNA quantifications of the samples. Figure 3.21 illustrates the amplification plot that shows the changes in fluorescence of SYBR green dye I versus cycle number of CYP2E1 gene of control and quercetin treated cells. In Figure 3.22, melting curve with one peak is represented for the detection of single PCR product.

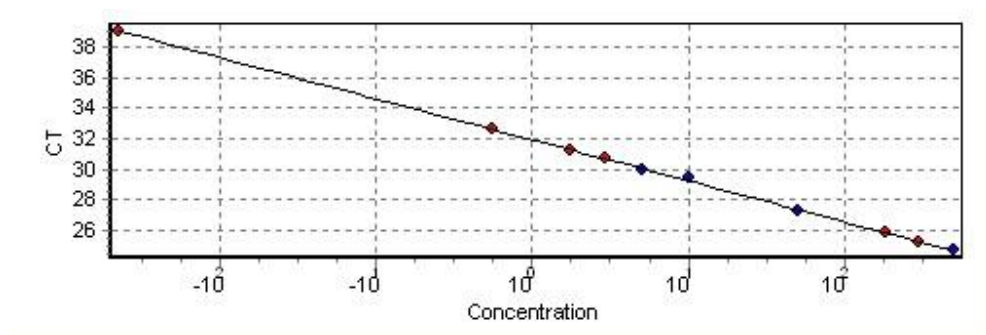


Figure 3.20 Standard curve generated from serial dilutions of control cDNA to calculate quantities of CYP2E1 mRNAs in the control and quercetin treated cells relatively.

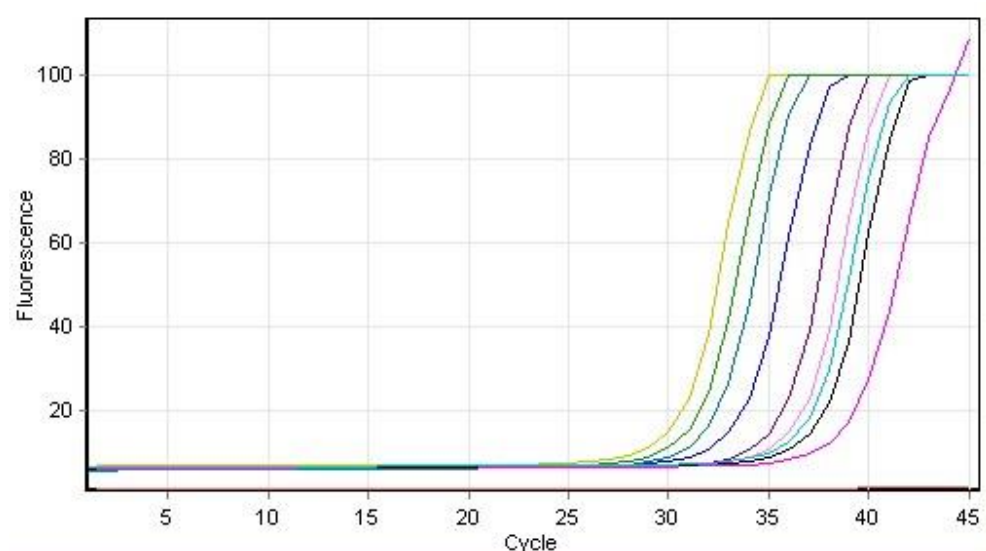


Figure 3.21 Amplification curve showing the accumulation of fluorescence emission at each reaction cycle.

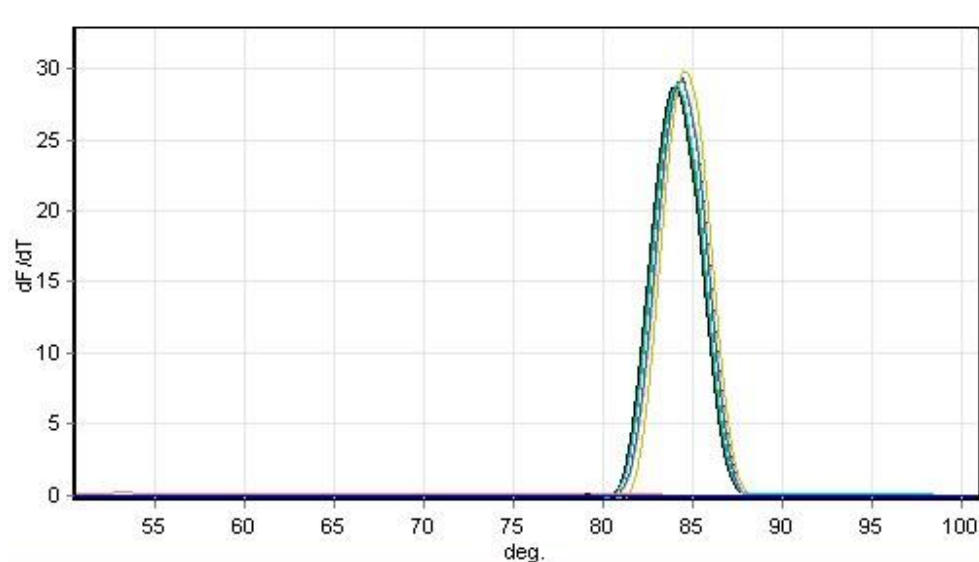


Figure 3.22 Melting curve showing the fluorescence emission change versus temperature. Detection of single peak means single PCR product.

The qRT-PCR products of CYP2E1 in control and quercetin treated SW620 colon carcinoma cells are given in Figure 3.23. Bands' positions on the gel overlaps with expected size of the CYP2E1 qRT-PCR product which is 184 bp.

The results were normalized with internal standard GAPDH. Livak method (Livak, 2001) was used to determine relative CYP2E1 mRNA expression in control and quercetin treated cells by using Ct values. Formulation for Livak ($2^{-\Delta\Delta Ct}$) method is given in Table 3.3. For calculation of relative mRNA expression by using Livak method, Ct values of control group were used as reference.



Figure 3.23 qRT-PCR products of CYP2E1 cDNA (184bp) of control (Lane 3-5) and quercetin treated (Lane 6-8) cells. 5 μ L of qRT-PCR product was loaded in each well. Lane 1 shows the bp markers and NTC (Lane 2) is the no template control.

Figure 3.24 shows the mean \pm SD of the relative CYP2E1 mRNA expressions of control and quercetin treated cells. The data was statistically analyzed by unpaired, two-tailed student's t-test.

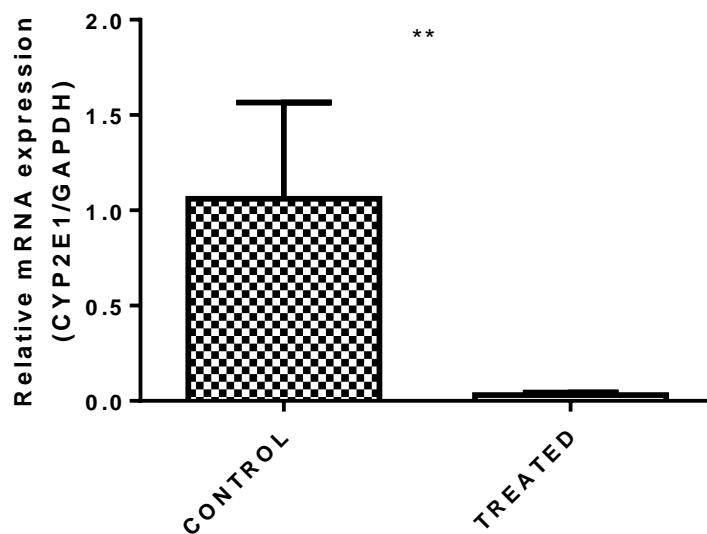


Figure 3.24 Comparison of CYP2E1 mRNA expressions between control and quercetin treated cells. The quantities are expressed as mean \pm SD of the relative expression. Experiments were carried out in triplicate. Statistical analysis of CYP2E1 mRNA expression was done by unpaired, two-tailed student's t-test.

3.4.4 GSTP1 mRNA Expression in the Control and the Quercetin Treated SW620 Cells

GSTP1 mRNA expression was determined by quantitative real time PCR (qRT-PCR) technique and GAPDH was used as internal standard to calculate relative mRNA expression of GSTP1. Specific annealing temperatures of the primers of GSTP1 and GAPDH given previously in Table 2.2 were used in qRT-PCR.

Figure 3.25 shows the standard curve which was generated from 1:10, 1:100, 1:500, 1:1000, and 1:5000 diluted cDNAs of the control cells used for mRNA quantifications of the samples. Figure 3.26 illustrates the amplification plot that shows the changes in fluorescence of SYBR green

dye I versus cycle number of GSTP1 gene of control and quercetin treated cells. In Figure 3.27, melting curve with one peak is represented for the detection of single PCR product.

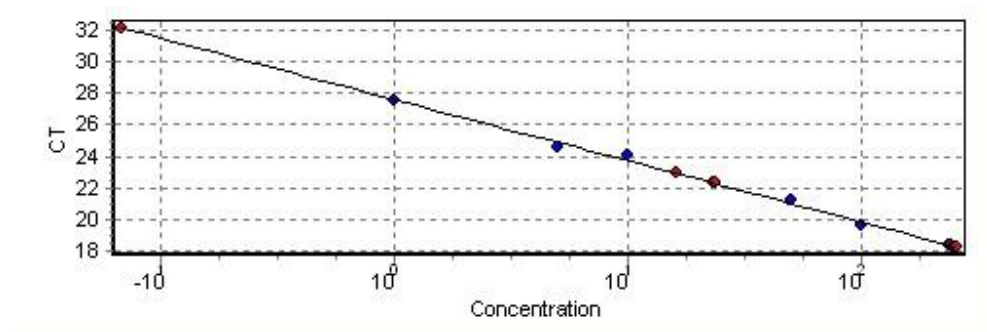


Figure 3.25 Standard curve generated from serial dilutions of control cDNA to calculate quantities of GSTP1 mRNAs in the control and quercetin treated cells relatively.

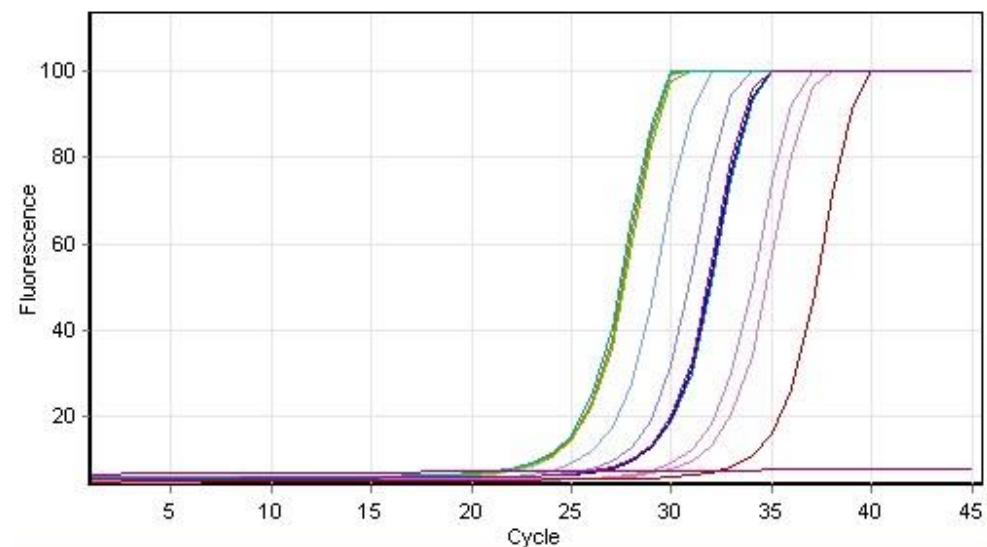


Figure 3.26 Amplification curve showing the accumulation of fluorescence emission at each reaction cycle.

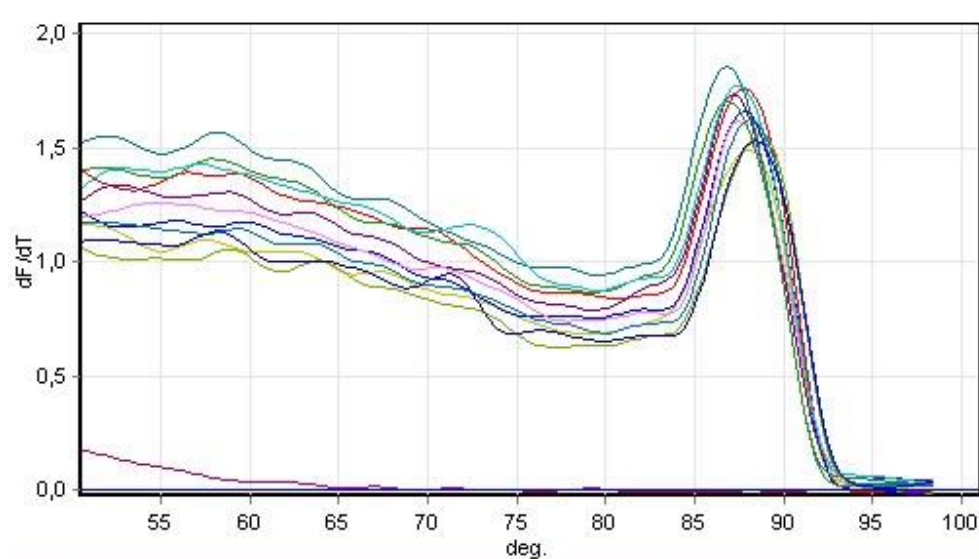


Figure 3.27 Melting curve showing the fluorescence emission change versus temperature. Detection of single peak means single PCR product.

The qRT-PCR products of GSTP1 in control and treated cells are given in Figure 3.28. Bands' positions on the gel overlap with expected size of the GSTP1 qRT-PCR products which is 137bp.

The results were normalized with internal standard GAPDH. Livak method (Livak, 2001) was used to determine relative GSTP1 mRNA expression in control and treated cells by using Ct values. Formulation for Livak ($2^{-\Delta\Delta Ct}$) method is given in Table 3.3. For calculation of relative mRNA expression by using Livak method, Ct values of control group were used as reference.

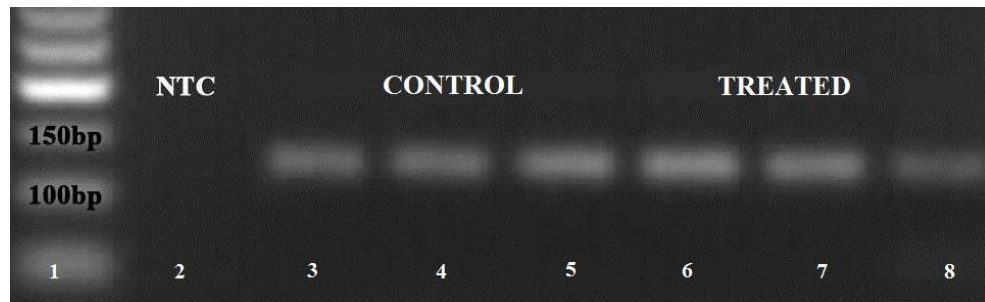


Figure 3.28 qRT-PCR products of GSTP1 cDNA (137bp) of control (Lane 3-5) and quercetin treated (Lane 6-8) cells. 5 μ L of qRT-PCR product was loaded in each well. Lane 1 shows the bp markers and NTC (Lane 2) is the no template control.

Figure 3.29 shows the mean \pm SD of the relative GSTP1 mRNA expressions of control and quercetin treated cells. The data was statistically analyzed by unpaired, two-tailed student's t-test.

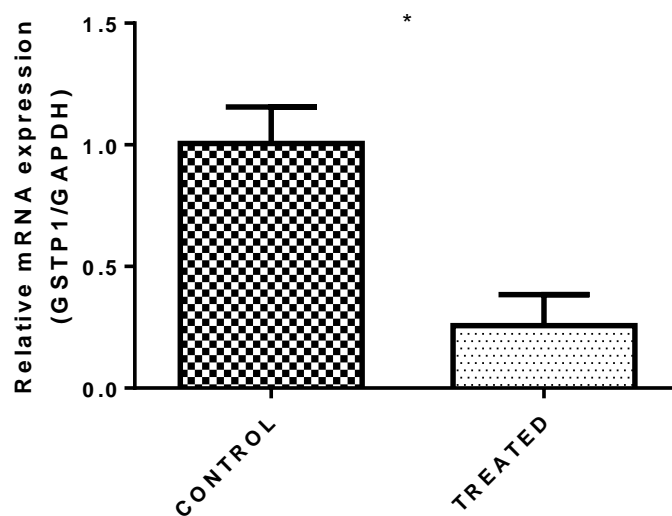


Figure 3.29 Comparison of GSTP1 mRNA expressions between control and quercetin treated cells. The quantities are expressed as mean \pm SD of the relative expression. Experiments were carried out in triplicate. Statistical analysis of GSTP1 mRNA expression was done by unpaired, two-tailed student's t-test and * means $P \leq 0.05$.

3.4.5 NQO1 mRNA Expression in the Control and the Quercetin Treated SW620 Cells

NQO1 mRNA expression was determined by quantitative real time PCR (qRT-PCR) technique and GAPDH was used as internal standard to calculate relative mRNA expression of NQO1. Specific annealing temperatures of the primers of NQO1 and GAPDH given previously in Table 2.2 were used in qRT-PCR.

Figure 3.30 shows the standard curve which was generated from 1:10, 1:100, 1:500, 1:1000, and 1:5000 diluted cDNAs of the control cells used for mRNA quantifications of the samples. Figure 3.31 illustrates the amplification plot that shows the changes in fluorescence of SYBR green dye I versus cycle number of NQO1 gene of control and quercetin treated cells. In Figure 3.32, melting curve with one peak is represented for the detection of single PCR product.

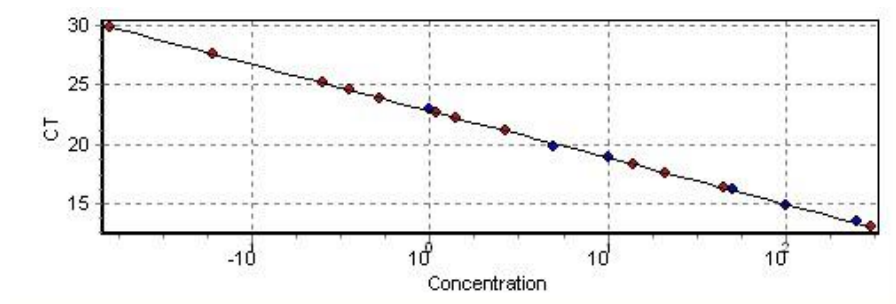


Figure 3.30 Standard curve generated from serial dilutions of control cDNA to calculate quantities of NQO1 mRNAs in the control and quercetin treated cells relatively.

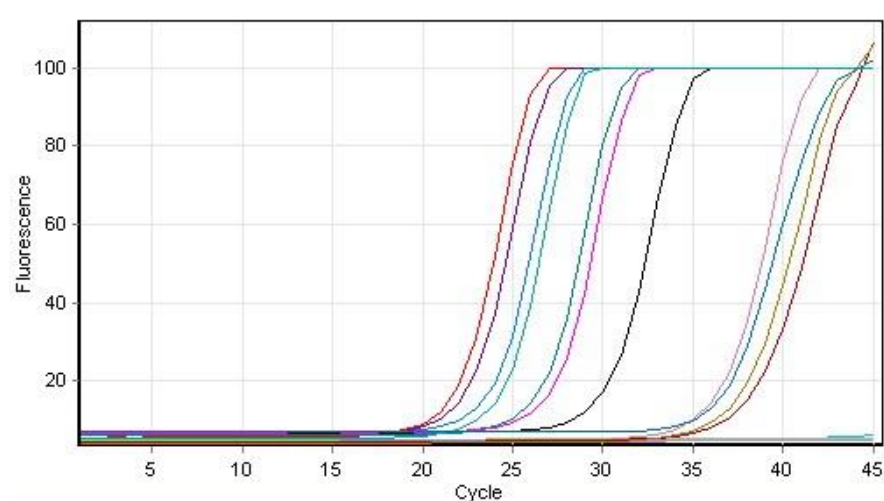


Figure 3.31 Amplification curve showing the accumulation of fluorescence emission at each reaction cycle.

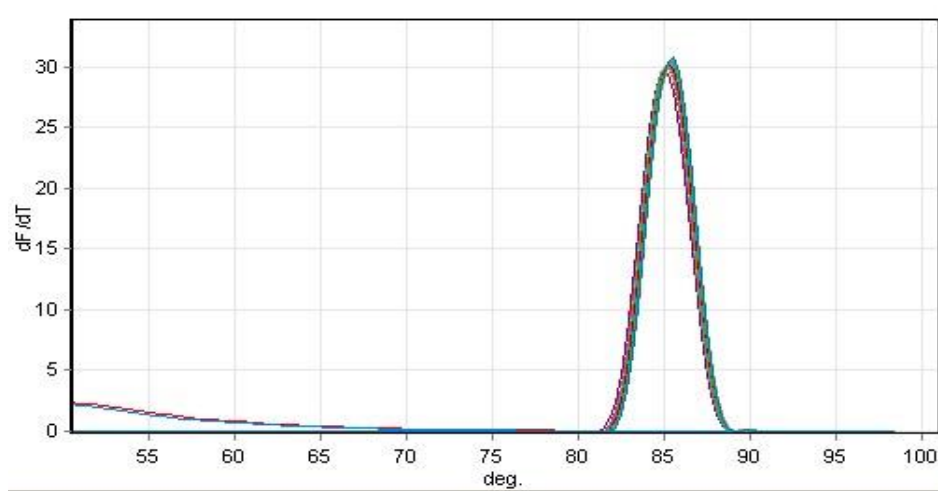


Figure 3.32 Melting curve showing the fluorescence emission change versus temperature. Detection of single peak means single PCR product.

The qRT-PCR products of NQO1 in control and quercetin treated SW620 colon carcinoma are given in Figure 3.33. Bands' positions on the gel overlaps with expected size of the NQO1 qRT-PCR products which 196bp.

The results were normalized with internal standard GAPDH. Livak method (Livak, 2001) was used to determine relative NQO1 mRNA expression in control and quercetin treated cells by using Ct values. Formulation for Livak ($2^{-\Delta\Delta Ct}$) method is given in Table 3.3. For calculation of relative mRNA expression by using Livak method, Ct values of control group were used as reference.



Figure 3.33 qRT-PCR products of NQO1 cDNA (196bp) of control and treated cells. 5 μ L of qRT-PCR product was loaded in each well. NTC is the no template control.

Figure 3.34 shows the mean \pm SD of the relative NQO1 mRNA expressions of control and treated cells. The data was statistically analyzed by unpaired, two-tailed student's t-test.

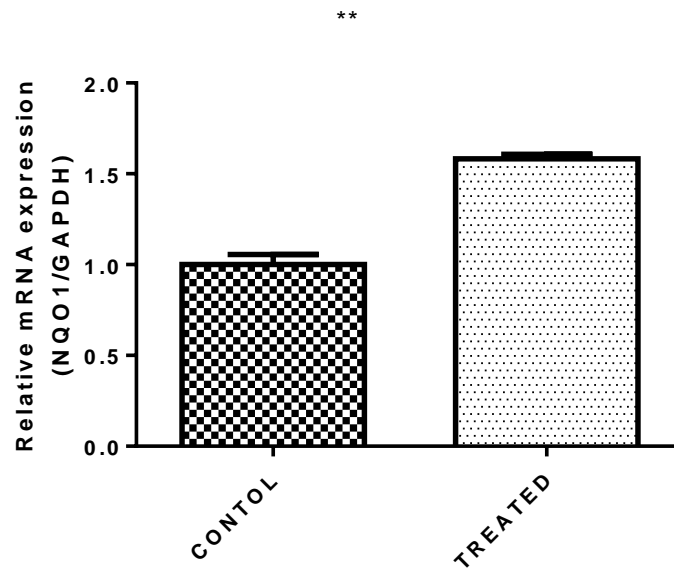


Figure 3.34 Comparison of NQO1 mRNA expressions between control and quercetin treated cells. The quantities are expressed as mean \pm SD of the relative expression. Experiments were carried out in triplicate. Statistical analysis of NQO1 mRNA expression was done by unpaired, two-tailed student's t-test. ** means $P \leq 0.01$.

CHAPTER 4

DISCUSSION

Cytochrome P450s are a heme-containing enzyme family, which catalyzing various oxidative, peroxidative, and reductive reactions including hydroxylations, epoxidations, N-dealkylations, O-dealkylations and S-oxidations. They have critical importance in the metabolism of xenobiotic substrates including therapeutic drugs, environmental pollutants and carcinogens and also in the metabolism of several endogenous compounds, such as bile acids, steroids and prostaglandins. CYPs catalyze the first step in metabolism of lipophilic xenobiotic by making them more hydrophilic (Lin and Lu, 1998). CYPs have a major role in therapeutic drug metabolism and bioinactivation, so induction and inhibition studies of these enzymes have a critical importance, especially in carcinogenicity studies. CYP1A1 and CYP2E1 are very important representatives of CYP family because of contributing notably to the production of DNA-adducts and activation of chemical carcinogens, respectively.

GSTs are phase II xenobiotic metabolizing enzymes, which perform the detoxification reactions of electrophilic xenobiotic compounds activated mostly by CYPs. They also detoxificate endogenous epoxides, hydroperoxides, and quinones formed as secondary metabolites during oxidative stress, through conjugation or reduction reactions (Hayes et al., 2005). NQO1 is another example for phase II xenobiotic metabolizing enzymes. It catalyzes the bioactivation of many quinone-based anticancer compounds (Simeone et al. 2003).

As previously mentioned, induction or inhibition of phase I and phase II xenobiotic metabolizing enzymes are very important especially in carcinogenicity studies and these enzymes, which are regulated transcriptionally, post-transcriptionally, translationally and post-translationally, have very complex regulation mechanisms. One of the main inducers and inhibitors of these enzymes are known to be plant phenolic compounds. The most studied family of these phenolic compounds is flavonoids. Flavonoids have been reported to exhibit anti-cancer, anti-viral, and anti-inflammatory effects, also they are known to reduce the risk of cardiovascular diseases (Nijveldt et al., 2001).

Quercetin is one of the most abundant flavonoids in fruits, vegetables, tea and wine, and its main sources are onions, apples, tea, and as a result readily available in the daily diet. Quercetin inhibits the proliferation of human cells from colon cancers (Agullo et al., 1994) and it is also known to influence the activity of the phase I and phase II enzymes to protect against cancer (Fischer and Fisher, 2000; Mikulcik and Fischer, 2001).

In present study, in vitro effects of plant phenolic quercetin on CYP1A1, CYP2E1, NQO1 and NQO1 protein and mRNA expressions on human colon carcinoma cell line SW620 were studied for the first time. In order to perform this, cells were grown and treated with 90 μ M (determined as IC50) quercetin prior to protein and RNA extraction. After 48 h from treatment, Alamar Blue (AB) assay was performed as described in the methods section and IC50 value of quercetin on SW620 cell line was found as 90 μ M. After cell culture studies protein and mRNA expression analysis of CYP1A1, CYP2E1, GSTP1 and NQO1 in control and quercetin treated SW620 colon carcinoma cells were performed to show the effects of quercetin at both translational and transcriptional levels (Table 4.1 and Table 4.2).

Table 4.1 Summary of the protein and mRNA expression analysis results for CYP1A1, CYP2E1, GSTP1 and NQO1 from control and quercetin treated cells.

	CYP1A1	CYP2E1	GSTP1	NQO1
	Protein expression (% of control)	Protein expression (% of control)	Protein expression (% of control)	Protein expression (% of control)
Quercetin Treated	53	83	65	71
	mRNA expression (% of control)	mRNA expression (% of control)	mRNA expression (% of control)	mRNA expression (% of control)
Quercetin Treated		3	25	160

According to these experimental results, plant phenolic quercetin caused 47 % and 17 % decrease in CYP1A1 and CYP2E1 protein expressions, respectively. As previously mentioned, CYP1A1 has a critical role in metabolic activation of chemical carcinogens and this role is very similar to the function of CYP2E1, which is involved in the activation of several carcinogens and other toxic chemicals. Previous studies have shown that quercetin is a ligand of the aryl hydrocarbon receptor (AhR), which regulates the transcriptional activity of CYP1A1 as previously mentioned (Williams et al., 2000). Another study (Zhou and Tang, 2005), which was conducted on several hepatic CYPs, has shown that quercetin had an inhibitory effect on CYP2E1 and this effect was based on noncompetitive mechanisms. In the light of these previous studies, one can easily say that

the protein expression results of present study on CYP1A1 and CYP2E1 are as expected and they are consistent with previous CYP enzyme studies.

Quercetin caused 85 % and 97 % decrease in CYP1A1 and CYP2E1 mRNA expressions, respectively. Quercetin has been shown to inhibit activation of nuclear factor-kappaB (NF-kB), which is a transcription factor regulates the transcription of several CYPs along with CYP1A1 and CYP2E1 (Kim et al., 2004) and our study confirmed this previous inhibitory effect of quercetin on CYP1A1 and CYP2E1 transcription. These decreased mRNA expression results are consistent with decreased protein expression results, however, it appears that transcriptional decrease is more drastic and it does not translate sharply into the protein expressions of CYP1A1 and CYP2E1. Consequently, according to these consistent mRNA and protein expression results in the present study, it appears that the inhibition effect of quercetin is both transcriptional and translational in CYP1A1 and CYP2E1 enzymes.

Experimental results have demonstrated that quercetin caused 35 % and 29 % decrease in GSTP1 and NQO1 protein expressions, respectively. As previously mentioned, GSTP1 catalyzes the conjugation of xenobiotic electrophiles with glutathione, and NQO1 reduces compounds with a quinone structure, so prevents the generation of toxic radicals and reactive oxygen species (ROS). There are strong evidences from *in vitro* and *in vivo* experiments that quercetin may affect phase II enzymes including GSTs and NQO1 (Valerio et al., 2001; Hayeshi et al., 2007; Wiegand et al., 2009; Al-Amro et al., 2014). The experimental findings of this study on GSTP1 and NQO1 protein expressions confirm the previous findings on this subject.

Quercetin caused 75 % decrease and 60 % increase in GSTP1 and NQO1 mRNA expressions respectively. Decrease in GSTP1 mRNA expression is coupled by a less drastic decrease protein expression level but still the

results for GSTP1 are consistent with each other and as expected in the lights of previous studies. On the other hand, NQO1 results for mRNA expression implies that the attempted increase in NQO1 mRNA expression does not translate into an increase in NQO1 protein expression. There are many experimental results that exhibit there is no correlation between mRNA and protein most of the time and only about 40 % of the protein levels are consistent with mRNA levels (Vogel et al., 2010; Schwanhausser, et. al., 2013). Schwanhausser et. al. suggested in their study that all mRNAs are not equal with regard to translation into proteins and only housekeeping genes have consistent results in mRNA and protein expression levels; however, other genes tend to have unstable proteins and mRNAs. There are several reasons for this inconsistency. Firstly, there are many complicated post-transcriptional mechanisms involved in translating mRNA into protein. Secondly, proteins have different half-lives and cells can control the protein degradation and synthesis (Greenbaum et al., 2003). Moreover, post-transcriptional regulations might be another reason for this lack of correlation. microRNA (miRNA) inhibition of target mRNA is a possible mechanism of post-transcriptional regulation. miRNAs are small, noncoding RNAs that affect numerous biological processes like mRNA degradation and inhibition of translation (Shengben et al., 2013). Since NQO1 mRNA expression was detected in present study, miRNA regulation was through inhibition of translation and there was no degradation of mRNA. miRNAs function in the form of miRNA-induced silencing complexes (miRISCs). Fabian *et al.*, described this inhibition and concluded that inhibition occurs through either initiation block or post-initiation block. Initiation blockage is the inhibition that miRISC acting as a repressor of cap recognition and prevents binding of 40S subunit or acting as 60S antagonist and prevents the binding of 60S subunit. In post-initiation blockage, miRISC makes ribosome to drop-off thus inhibits the ribosomal elongation. Figure 4.1 represents the schematic illustration of translational inhibition by miRNA.

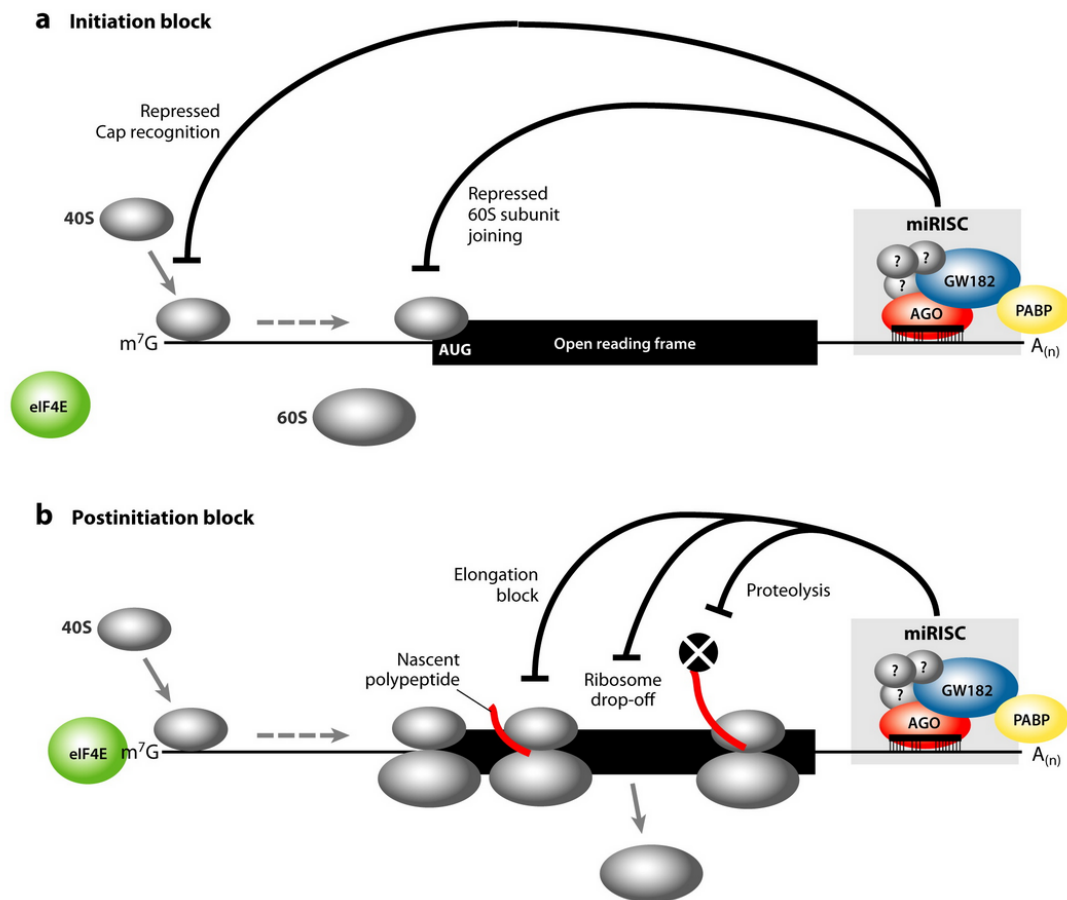


Figure 4.1 Two different mechanisms for translational inhibition by miRNAs (Fabian *et al.*, 2010).

In conclusion, the results of this study showed that plant phenolic quercetin can modulate the progression of colon carcinoma by affecting the expression of protein and mRNA of xenobiotic metabolizing phase I and phase II enzymes CYP1A1, CYP2E1, GSTP1 and NQO1. Nevertheless, all four of these enzymes have different expression levels on different cell lines, further studies on different colon carcinoma cell lines along with *in vivo* studies are required in order to conclude that quercetin has significant effects on colon carcinoma.

CHAPTER 5

CONCLUSION

As mentioned earlier, this study is the first *in vitro* study that uses the SW-620 colon cancer cell line to test the effect of plant phenolic quercetin on the protein and mRNA expression of xenobiotic metabolizing phase I and phase II enzymes – CYP1A1, CYP2E1, GSTP1 and NQO1.

In order to perform this study, cells were grown and treated with 90 μ M (determined as IC₅₀) quercetin prior to protein and RNA extraction. After cell culture studies protein and mRNA expression analysis of CYP1A1, CYP2E1, GSTP1 and NQO1 in control and quercetin treated SW620 colon carcinoma cells were performed to show the effects of quercetin at both translational and transcriptional levels.

Quercetin treatment caused 47 % decrease in CYP1A1 protein expression ($p < 0.01$) and 17 % decrease in CYP2E1 protein expression ($p < 0.01$). Furthermore, quercetin treatment caused 85 % decrease in CYP1A1 mRNA expression and 97 % decrease in CYP2E1 mRNA expression with respect to control cells and results are normalized with GAPDH as an internal reference. Moreover, quercetin treatment also caused 35 % decrease in GSTP1 protein expression ($p < 0.001$) and 29 % decrease in NQO1 protein expression ($p < 0.001$). In addition, quercetin treatment caused 75 % decrease in GSTP1 mRNA expression ($p < 0.05$), whereas NQO1 mRNA expression is increased 1.6 fold ($p < 0.01$) after quercetin treatment.

In conclusion, the results of this study showed that plant phenolic quercetin can modulate the progression of colon carcinoma by affecting the expression of protein and mRNA of xenobiotic metabolizing phase I and phase II enzymes CYP1A1, CYP2E1, GSTP1 and NQO1. However, all four of these enzymes have different expression levels on different cell lines, further studies on different colon carcinoma cell lines along with *in vivo* studies are required in order to conclude that quercetin has significant effects on colon carcinoma. In the light of these findings of present study, future researches can be done in order to understand the association between the consumption of a plant phenolic and lowered cancer risk. Nevertheless, the results of the present study support the hypothesis that quercetin may be involved in the prevention of colon carcinoma, by reducing the carcinogen formation through inhibition of xenobiotic metabolizing enzymes such as CYP1A1, CYP2E1, GSTP1 and NQO1 which are known to be involved in pro-carcinogen activation.

REFERENCES

- Adali, O., Carver, G. C., & Philpot, R. M. (1998). Modulation of human flavin-containing monooxygenase 3 activity by tricyclic antidepressants and other agents: importance of residue 428. *Arch Biochem Biophys*, 358(1), 92-97.
- Agullo, G., Gamet, L., Besson, C., Demigne, C., & Remesy, C. (1994). Quercetin exerts a preferential cytotoxic effect on active dividing colon carcinoma HT29 and Caco-2 cells. *Cancer Lett*, 87(1), 55-63.
- Androutsopoulos, V. P., Tsatsakis, A. M., & Spandidos, D. a. (2009). Cytochrome P450 CYP1A1: wider roles in cancer progression and prevention. *BMC Cancer*, 9, 187.
- Arinç, E., Adalı, O., İşcan, M. and Güray, T. (1991). Stimulatory effects of benzene on rabbit liver and kidney microsomal cytochrome P-450 drug metabolizing enzymes. *Archives of Toxicology*, 65, 186-190
- Arinç, E., Adalı, O., & Gençler-Ozkan, A. M. (2000a). Induction of N-nitrosodimethylamine metabolism in liver and lung by in vivo pyridine treatments of rabbits. *Archives of Toxicology*, 74(6), 329–34.
- Arinç, E., Adalı, O., & Gençler-Özkan, A. M. (2000b). Stimulation of aniline, *p*-nitrophenol and N-nitrosodimethylamine metabolism in kidney by pyridine pretreatment of rabbits. *Archives of Toxicology*, 74(9), 527–532.

- Arinç E., Arslan S. and Adalı O. (2005) Differential effects of diabetes on CYP2E1 and CYP2B4 proteins and associated drug metabolizing enzyme activities in rabbit liver. *Archives of Toxicology*, 79, 427-433
- Arinç, E., Arslan, S., Bozcaarmutlu, A., & Adali, O. (2007). Effects of diabetes on rabbit kidney and lung CYP2E1 and CYP2B4 expression and drug metabolism and potentiation of carcinogenic activity of N-nitrosodimethylamine in kidney and lung. *Food and Chemical Toxicology*, 45(1), 107–118.
- Arinç, E., Arslan, Ş., & Adalı, O. (2005). Differential effects of diabetes on CYP2E1 and CYP2B4 proteins and associated drug metabolizing enzyme activities in rabbit liver. *Archives of Toxicology*, 79(8), 427–433.
- Asher, G., Dym, O., Tsvetkov, P., Adler, J., & Shaul, Y. (2006). The crystal structure of NAD(P)H quinone oxidoreductase 1 in complex with its potent inhibitor dicoumarol. *Biochemistry*, 45(20), 6372-6378.
- Bertz, R. J., & Granneman, G. R. (1997). Use of in vitro and in vivo data to estimate the likelihood of metabolic pharmacokinetic interactions. *Clin Pharmacokinet*, 32(3), 210-258.
- Bondonno, C. P., Croft, K. D., Ward, N., Considine, M. J., & Hodgson, J. M. (2015). Dietary flavonoids and nitrate: effects on nitric oxide and vascular function. *Nutr Rev*, 73(4), 216-235.
- Bravo, L. (1998). Polyphenols: chemistry, dietary sources, metabolism, and nutritional significance. *Nutr Rev*, 56(11), 317-333.
- Cavelier, G., & Amzel, L. M. (2001). Mechanism of NAD(P)H:quinone reductase: Ab initio studies of reduced flavin. *Proteins*, 43(4), 420-432.

- Celik, S. E., Ozyurek, M., Guclu, K., Capanoglu, E., & Apak, R. (2014). Identification and anti-oxidant capacity determination of phenolics and their glycosides in elderflower by on-line HPLC-CUPRAC method. *Phytochem Anal*, 25(2), 147-154.
- Caro, Andres A., & Cederbaum, Arthur I. (2006). Role of Phosphatidylinositol 3-Kinase/AKT as a Survival Pathway against CYP2E1-Dependent Toxicity. *Journal of Pharmacology and Experimental Therapeutics*, 318(1), 360-372. doi: 10.1124/jpet.106.102921
- Chen, S., Wu, K., Zhang, D., Sherman, M., Knox, R., & Yang, C. S. (1999). Molecular characterization of binding of substrates and inhibitors to DT-diaphorase: combined approach involving site-directed mutagenesis, inhibitor-binding analysis, and computer modeling. *Mol Pharmacol*, 56(2), 272-278.
- Cheung, K. L., & Kong, A. N. (2009). Molecular targets of dietary phenethyl isothiocyanate and sulforaphane for cancer chemoprevention. *AAPS J*, 12(1), 87-97.
- Choi, J. A., Kim, J. Y., Lee, J. Y., Kang, C. M., Kwon, H. J., Yoo, Y. D., . . . Lee, S. J. (2001). Induction of cell cycle arrest and apoptosis in human breast cancer cells by quercetin. *Int J Oncol*, 19(4), 837-844.
- De Waziers, I, Cugnenc, P H, Yang, C S, Leroux, J P, & Beaune, P H. (1990). Cytochrome P 450 isoenzymes, epoxide hydrolase and glutathione transferases in rat and human hepatic and extrahepatic

tissues. *Journal of Pharmacology and Experimental Therapeutics*, 253(1), 387-394.

Denda, A., Endoh, T., Tang, Q., Tsujiuchi, T., Nakae, D., & Konishi, Y. (1998). Prevention by inhibitors of arachidonic acid cascade of liver carcinogenesis, cirrhosis and oxidative DNA damage caused by a choline-deficient, L-amino acid-defined diet in rats. *Mutat Res*, 402(1-2), 279-288.

Diamond L., Sardet C. & Rothblat G.H. (1968) The metabolims of 7, 12-dimethyl-benz (1) anthracene in cell cultures. *Int. J. Cancer*, 3 : 838-849.

Dills, R. L., & Klaassen, C. D. (1986). The effect of inhibitors of mitochondrial energy production on hepatic glutathione, UDP-glucuronic acid, and adenosine 3'-phosphate-5'-phosphosulfate concentrations. *Drug Metab Dispos*, 14(2), 190-196.

Ding, X., & Kaminsky, L. S. (2003). Human extrahepatic cytochromes P450: function in xenobiotic metabolism and tissue-selective chemical toxicity in the respiratory and gastrointestinal tracts. *Annu Rev Pharmacol Toxicol*, 43, 149-173.

Fabian, Marc Robert, Sonenberg, Nahum, & Filipowicz, Witold. (2010). Regulation of mRNA Translation and Stability by microRNAs. *Annual Review of Biochemistry*, 79(1), 351-379. doi:doi:10.1146/annurev-biochem-060308-103103

- Farkas, O., Jakus, J., & Heberger, K. (2004). Quantitative structure-antioxidant activity relationships of flavonoid compounds. *Molecules*, 9(12), 1079-1088.
- Fujita, K., & Kamataki, T. (2001). Role of human cytochrome P450 (CYP) in the metabolic activation of N-alkylnitrosamines: application of genetically engineered *Salmonella typhimurium* YG7108 expressing each form of CYP together with human NADPH-cytochrome P450 reductase. *Mutat Res*, 483(1-2), 35-41.
- Galijatovic, A., Beaton, D., Nguyen, N., Chen, S., Bonzo, J., Johnson, R., . . . Tukey, R. H. (2004). The human CYP1A1 gene is regulated in a developmental and tissue-specific fashion in transgenic mice. *J Biol Chem*, 279(23), 23969-23976.
- Greenbaum, D., Colangelo, C., Williams, K., & Gerstein, M. (2003). Comparing protein abundance and mRNA expression levels on a genomic scale. *Genome Biol*, 4(9), 117.
- Guengerich, F. P. (1992). Characterization of human cytochrome P450 enzymes. *FASEB J*, 6(2), 745-748.
- Guengerich, F. P. (2001). Common and uncommon cytochrome P450 reactions related to metabolism and chemical toxicity. *Chemical Research in Toxicology*, 14(6), 611-50.
- Guengerich, F. P. (2003). Cytochromes P450, drugs, and diseases. *Mol Interv*, 3(4), 194-204.
- Halpert, J. R., Domanski, T. L., Adali, O., Biagini, C. P., Cosme, J., Dierks, E. A., . . . Zheng, Z. (1998). Structure-function of cytochromes P450

and flavin-containing monooxygenases: implications for drug metabolism. *Drug Metab Dispos*, 26(12), 1223-1231.

Hammons, G. J., Milton, D., Stepps, K., Guengerich, F. P., Tukey, R. H., & Kadlubar, F. F. (1997). Metabolism of carcinogenic heterocyclic and aromatic amines by recombinant human cytochrome P450 enzymes. *Carcinogenesis*, 18(4), 851-854.

Hankinson, O. (1995). The aryl hydrocarbon receptor complex. *Annu Rev Pharmacol Toxicol*, 35, 307-340.

Hayes, J. D., McLeod, R., Ellis, E. M., Pulford, D. J., Ireland, L. S., McLellan, L. I., ... & Neal, G. E. (1995). Regulation of glutathione S-transferases and aldehyde reductase by chemoprotectors: studies of mechanisms responsible for inducible resistance to aflatoxin B1. IARC scientific publications, (139), 175-187.

Hayes, J. D., Flanagan, J. U., & Jowsey, I. R. (2005). Glutathione transferases. *Annu. Rev. Pharmacol. Toxicol.*, 45, 51-88.

Hertog, M. G., Hollman, P. C., Katan, M. B., & Kromhout, D. (1993). Intake of potentially anticarcinogenic flavonoids and their determinants in adults in The Netherlands. *Nutr Cancer*, 20(1), 21-29.

Hollman, P. C., van Trijp, J. M., Mengelers, M. J., de Vries, J. H., & Katan, M. B. (1997). Bioavailability of the dietary antioxidant flavonol quercetin in man. *Cancer Lett*, 114(1-2), 139-140.

- Hose, C. D., Hollingshead, M., Sausville, E. A., & Monks, A. (2003). Induction of CYP1A1 in tumor cells by the antitumor agent 2-[4-amino-3-methylphenyl]-5-fluoro-benzothiazole: a potential surrogate marker for patient sensitivity. *Mol Cancer Ther*, 2(12), 1265-1272.
- Huber, W. W., McDaniel, L. P., Kaderlik, K. R., Teitel, C. H., Lang, N. P., & Kadlubar, F. F. (1997). Chemoprotection against the formation of colon DNA adducts from the food-borne carcinogen 2-amino-1-methyl-6-phenylimidazo[4,5-b]pyridine (PhIP) in the rat. *Mutat Res*, 376(1-2), 115-122.
- Huggins, C., & Fukunishi, R. (1964). Mammary and peritoneal tumors induced by intraperitoneal administration of 7, 12-dimethylbenz [a] anthracene in newborn and adult rats. *Cancer Research*, 23(5), 785-789.
- Jaiswal, A. K., Gonzalez, F. J., & Nebert, D. W. (1985). Human P1-450 gene sequence and correlation of mRNA with genetic differences in benzo[a]pyrene metabolism. *Nucleic Acids Res*, 13(12), 4503-4520.
- Kawajiri, K., Watanabe, J., Gotoh, O., Tagashira, Y., Sogawa, K., & Fujii-Kuriyama, Y. (1986). Structure and drug inducibility of the human cytochrome P-450c gene. *Eur J Biochem*, 159(2), 219-225.
- Khanduja, K. L., Gandhi, R. K., Pathania, V., & Syal, N. (1999). Prevention of N-nitrosodiethylamine-induced lung tumorigenesis by ellagic acid and quercetin in mice. *Food Chem Toxicol*, 37(4), 313-318.
- Kinoshita, N., & Gelboin, H. V. (1972). Aryl hydrocarbon hydroxylase and polycyclic hydrocarbon tumorigenesis: effect of the enzyme

inhibitor 7,8-benzoflavone on tumorigenesis and macromolecule binding. *Proc Natl Acad Sci U S A*, 69(4), 824-828.

Klingenberg, M. (1958). Pigments of rat liver microsomes. *Archives of biochemistry and biophysics*, 75(2), 376-386.

Knutson, J. R., Walbridge, D. G., & Brand, L. (1982). Decay-associated fluorescence spectra and the heterogeneous emission of alcohol dehydrogenase. *Biochemistry*, 21(19), 4671-4679.

Laemmli, U. K. (1970). Cleavage of structural proteins during the assembly of the head of bacteriophage T4. *nature*, 227(5259), 680-685.

Leong, C. O., Gaskell, M., Martin, E. A., Heydon, R. T., Farmer, P. B., Bibby, M. C. Stevens, M. F. (2003). Antitumour 2-(4-aminophenyl)benzothiazoles generate DNA adducts in sensitive tumour cells in vitro and in vivo. *Br J Cancer*, 88(3), 470-477.

Lin, J. H., & Lu, A. Y. (1998). Inhibition and induction of cytochrome P450 and the clinical implications. *Clinical pharmacokinetics*, 35(5), 361-390.

Li, L., Yu, M., Chin, R., Lucksiri, A., Flockhart, D. A., & Hall, S. D. (2007). Drug-drug interaction prediction: a Bayesian meta-analysis approach. *Stat Med*, 26(20), 3700-3721.

Li, Shengben, Liu, Lin, Zhuang, Xiaohong, Yu, Yu, Liu, Xigang, Cui, Xia, Chen, Xuemei. MicroRNAs Inhibit the Translation of Target mRNAs on the Endoplasmic Reticulum in Arabidopsis. *Cell*, 153(3), 562-574.

- Lieber, C. S. (1997). Cytochrome P-450E1: its physiological and pathological role. *Physiological reviews*, 77(2), 517-544.
- Middleton, E., Jr. (1998). Effect of plant flavonoids on immune and inflammatory cell function. *Adv Exp Med Biol*, 439, 175-182.
- Nebert, D. W., & Gonzalez, F. J. (1985). Cytochrome P450 gene expression and regulation. *Trends in Pharmacological Sciences*, 6, 160-164.
- Nebert, D. W., & Gonzalez, F. J. (1987). P450 genes: structure, evolution, and regulation. *Annual review of biochemistry*, 56(1), 945-993.
- Nebert, D. W., & Russell, D. W. (2002). Clinical importance of the cytochromes P450. *The Lancet*, 360(9340), 1155-1162.
- Nelson, D. R., Koymans, L., Kamataki, T., Stegeman, J. J., Feyereisen, R., Waxman, D. J., . . . Nebert, D. W. (1996). P450 superfamily: update on new sequences, gene mapping, accession numbers and nomenclature. *Pharmacogenetics*, 6(1), 1-42.
- Nijveldt, R. J., van Nood, E., van Hoorn, D. E., Boelens, P. G., van Norren, K., & van Leeuwen, P. A. (2001). Flavonoids: a review of probable mechanisms of action and potential applications. *Am J Clin Nutr*, 74(4), 418-425.
- Omura, T. (1999). Forty years of cytochrome P450. *Biochem Biophys Res Commun*, 266(3), 690-698.

- Oneta, C. M., Lieber, C. S., Li, J., Rüttimann, S., Schmid, B., Lattmann, J., ... & Seitz, H. K. (2002). Dynamics of cytochrome P4502E1 activity in man: induction by ethanol and disappearance during withdrawal phase. *Journal of hepatology*, 36(1), 47-52.
- Pandey, K. B., & Rizvi, S. I. (2009). Plant polyphenols as dietary antioxidants in human health and disease. *Oxid Med Cell Longev*, 2(5), 270-278.
- Porubsky, P. R., Meneely, K. M., & Scott, E. E. (2008). Structures of human cytochrome P-450 2E1. Insights into the binding of inhibitors and both small molecular weight and fatty acid substrates. *J Biol Chem*, 283(48), 33698-33707
- Raunio, H., Husgafvel-Pursiainen, K., Anttila, S., Hietanen, E., Hirvonen, A., & Pelkonen, O. (1995). Diagnosis of polymorphisms in carcinogen-activating and inactivating enzymes and cancer susceptibility--a review. *Gene*, 159(1), 113-121
- Ross, J. F., Chaudhuri, P. K., & Ratnam, M. (1994). Differential regulation of folate receptor isoforms in normal and malignant tissues in vivo and in established cell lines. Physiologic and clinical implications. *Cancer*, 73(9), 2432-2443.
- Ross, D. T., Scherf, U., Eisen, M. B., Perou, C. M., Rees, C., Spellman, P., ... & Brown, P. O. (2000). Systematic variation in gene expression patterns in human cancer cell lines. *Nature genetics*, 24(3), 227-235.
- Safe, S. (1990). Polychlorinated biphenyls (PCBs), dibenzo-p-dioxins (PCDDs), dibenzofurans (PCDFs), and related compounds:

environmental and mechanistic considerations which support the development of toxic equivalency factors (TEFs). *Crit Rev Toxicol*, 21(1), 51-88.

Sampson, L., Rimm, E., Hollman, P. C., de Vries, J. H., & Katan, M. B. (2002). Flavonol and flavone intakes in US health professionals. *J Am Diet Assoc*, 102(10), 1414-1420.

Scambia, G., Panici, P. B., Ranelletti, F. O., Ferrandina, G., De Vincenzo, R., Piantelli, M., . . . Mancuso, S. (1994). Quercetin enhances transforming growth factor beta 1 secretion by human ovarian cancer cells. *Int J Cancer*, 57(2), 211-215.

Schlager, J. J., & Powis, G. (1990). Cytosolic NAD(P)H:(quinone-acceptor)oxidoreductase in human normal and tumor tissue: effects of cigarette smoking and alcohol. *Int J Cancer*, 45(3), 403-409.

Schmidt, J. V., & Bradfield, C. A. (1996). Ah receptor signaling pathways. *Annu Rev Cell Dev Biol*, 12, 55-89.

Schwanhausser, B., Busse, D., Li, N., Dittmar, G., Schuchhardt, J., Wolf, J., . . . Selbach, M. (2013). Corrigendum: Global quantification of mammalian gene expression control. *Nature*, 495(7439), 126-127.

Sen, A., & Arinc, E. (1997). Separation of three P450 isozymes from liver microsomes of gilthead seabream treated with beta-NF and partial purification of cytochrome P4501A1. *Biochem Mol Biol Int*, 41(1), 131-141.

- Siess, M. H., Le Bon, A. M., Canivenc-Lavier, M. C., & Suschetet, M. (2000). Mechanisms involved in the chemoprevention of flavonoids. *Biofactors*, *12*(1-4), 193-199.
- Simeone, A. M., Broemeling, L. D., Rosenblum, J., & Tari, A. M. (2003). HER2/neu reduces the apoptotic effects of N-(4-hydroxyphenyl)retinamide (4-HPR) in breast cancer cells by decreasing nitric oxide production. *Oncogene*, *22*(43), 6739-6747.
- Tew, K. D., & Townsend, D. M. (2011). Regulatory functions of glutathione S-transferase P1-1 unrelated to detoxification. *Drug Metab Rev*, *43*(2), 179-193
- Thor, H., Smith, M. T., Hartzell, P., Bellomo, G., Jewell, S. A., & Orrenius, S. (1982). The metabolism of menadione (2-methyl-1,4-naphthoquinone) by isolated hepatocytes. A study of the implications of oxidative stress in intact cells. *J Biol Chem*, *257*(20), 12419-12425.
- Towbin, H., Staehelin, T., & Gordon, J. (1979). Electrophoretic transfer of proteins from polyacrylamide gels to nitrocellulose sheets: procedure and some applications. *Proceedings of the National Academy of Sciences of the United States of America*, *76*(9), 4350-4354.
- Townsend, D. M., & Tew, K. D. (2003). The role of glutathione-S-transferase in anti-cancer drug resistance. *Oncogene*, *22*(47), 7369-75.
- Valerio, L. G., Jr., Kepa, J. K., Pickwell, G. V., & Quattrochi, L. C. (2001). Induction of human NAD(P)H:quinone oxidoreductase (NQO1) gene expression by the flavonol quercetin. *Toxicol Lett*, *119*(1), 49-57.

- Vogel, C., Abreu Rde, S., Ko, D., Le, S. Y., Shapiro, B. A., Burns, S. C., . . . Penalva, L. O. (2010). Sequence signatures and mRNA concentration can explain two-thirds of protein abundance variation in a human cell line. *Mol Syst Biol*, 6, 400.
- Walsh, A. A., Szklarz, G. D., & Scott, E. E. (2013). Human cytochrome P450 1A1 structure and utility in understanding drug and xenobiotic metabolism. *J Biol Chem*, 288(18), 12932-12943.
- Wang, W., & Higuchi, C. M. (1995). Induction of NAD(P)H:quinone reductase by vitamins A, E and C in Colo205 colon cancer cells. *Cancer Lett*, 98(1), 63-69.
- Wu, B., & Dong, D. (2012). Human cytosolic glutathione transferases: structure, function, and drug discovery. *Trends Pharmacol Sci*, 33(12), 656-668.
- Yang, C. S., Brady, J. F., & Hong, J. Y. (1992). Dietary effects on cytochromes P450, xenobiotic metabolism, and toxicity. *FASEB J*, 6(2), 737-744.